


Review

Open Access



Recent advancement of solid oxide fuel cells towards semiconductor membrane fuel cells

Monika Singh^{1,2,#,*}, Sara Paydar^{3,#}, Akhilesh Kumar Singh¹, Ranjan Singhal⁴ , Aradhana Singh⁵, Manish Singh^{4,6,*} 

¹School of Materials Science & Technology, Indian Institute of Technology, Banaras Hindu University, Varanasi 221005, India.

²Department of Chemistry, University of Calgary, Calgary, AB T2N 1N4, Canada.

³Institute of Chemistry, University of Tartu, Tartu 50411, Estonia.

⁴School of Materials Science and Engineering, Oklahoma State University, Tulsa, Ok 74106, USA.

⁵Laboratory of Air Pollution and Global Climate Change, Department of Botany, Banaras Hindu University, Varanasi 221005, India.

⁶Department of Metallurgical and Materials Engineering, Indian Institute of Technology Patna, Bihar 801106, India.

#Authors contributed equally.

***Correspondence to:** Dr. Monika Singh, Department of Chemistry, University of Calgary, Calgary, AB T2N 1N4, Canada. E-mail: monikas.rs.mst15@itbhu.ac.in; Dr. Manish Singh, Department of Metallurgical and Materials Engineering, Indian Institute of Technology Patna, Bihta, Bihar 801106, India. E-mail: manish.singh@iitp.ac.in

How to cite this article: Singh M, Paydar S, Singh AK, Singhal R, Singh A, Singh M. Recent advancement of solid oxide fuel cells towards semiconductor membrane fuel cells. *Energy Mater* 2024;4:400012. <https://dx.doi.org/10.20517/energymater.2023.54>

Received: 17 Jul 2023 **First Decision:** 11 Aug 2023 **Revised:** 2 Oct 2023 **Accepted:** 13 Dec 2023 **Published:** 17 Jan 2024

Academic Editor: Bin Wang **Copy Editor:** Fangyuan Liu **Production Editor:** Fangyuan Liu

Abstract

In the last few decades, there has been remarkable progress in the development of solid oxide fuel cells (SOFCs) based on both traditional solid electrolyte materials and novel semiconductor membranes. However, limited attention has been given to the transition of SOFCs from oxide ion-based electrolyte membranes to semiconductor membrane devices, considering the overall perspective of materials, technology, and scientific principles. Traditional knowledge strictly dictates that semiconductors should not be used as the membrane unless these materials possess negligible electronic conduction. This is because semiconductor membrane materials typically exhibit significantly higher electrical conductivity, surpassing the inherent ionic conductivity. Interestingly, by using semiconductors as the membrane, numerous novel materials have been demonstrated in the literature, which seems difficult to understand from traditional SOFC knowledge. Therefore, there is an emerging need to summarize and explore new understanding and knowledge of materials, technology, and science of SOFCs and Semiconductor Membrane Fuel Cells and their transition. In this review, we attempted to summarize the gap between the current state of SOFCs and the advancements in new materials, technologies, scientific principles, and mechanisms driving the development of such devices.

Keywords: Solid oxide fuel cell, semiconductor membrane fuel cells, band alignment, built-in electric field, ceramic fuel cell



© The Author(s) 2024. **Open Access** This article is licensed under a Creative Commons Attribution 4.0 International License (<https://creativecommons.org/licenses/by/4.0/>), which permits unrestricted use, sharing, adaptation, distribution and reproduction in any medium or format, for any purpose, even commercially, as long as you give appropriate credit to the original author(s) and the source, provide a link to the Creative Commons license, and indicate if changes were made.



INTRODUCTION

The rapid depletion of fossil energy resources (coal, oil, natural gas, *etc.*) is causing a pressing need for the efficient utilization of green energy to support human activities, fast economic growth, and industrial development. Moreover, it has been recognized that considering fossil energy resources as a long-term energy solution has adversely affected the environment, chiefly due to the emission of greenhouse and other harmful gases^[1]. However, the emergent concerns over the limited stock of conventional energy sources, consequent constant emission of global warming gases, and unbalanced price and supply have caused progressive interest in the development of unconventional renewable energy technologies with high efficiency and less environmental damage. In this energetic perspective, hydroelectric, wind power, solar power, wave power, geothermal, and bio-energy technologies are being considered and executed as alternative approaches for electricity generation and combustion-free energy sources. On the one side, they will have a considerable influence on the global energy landscape and the weather challenge, and on the other side, they continue to struggle with extreme investment expenses and longevity issues because of the congenital intricate cell structure and demanding materials and fabrication necessities^[2]. Thus, among the existing capable sustainable technologies, solid oxide fuel cells (SOFCs) are considered to be better choices due to their exceptional efficiency in converting fuels to electricity, multi-fuel compatibility, low pollutant emissions, and their potential to directly employ existing fossil energy resources or renewable biofuels. However, despite having numerous advantages, the high operating temperature range and high production cost, owing to the use of expensive materials, pose a significant hindrance to the marketing of SOFC technology. Thus, the commercialization barrier has remained unresolved, and there is still a sustained journey to go before widespread implementation^[3]. Therefore, innovative functional materials and novel system designs are needed to expedite the commercialization of SOFCs.

SOFCs: conventional electrolyte to semiconductor membranes

SOFCs are classified into three kinds based on cell operating temperatures. Firstly, high-temperature SOFCs (HT-SOFCs) were developed in the initial development that worked at high temperatures in the range of 900-1,000 °C. A high operating temperature is required to ensure adequate ionic conductivity. On the one hand, a high working temperature improves the reaction rates and charge conduction; on the other hand, it possesses critical hurdles for practical applications such as high material cost, material degradation, and other challenges for material compatibility. Therefore, after so much effort, intermediate temperature SOFCs (IT-SOFCs) were developed to reduce the operating temperature, which can work at a temperature range from 650 to 800 °C. Moreover, nanostructured materials are currently well-preferred, particularly at low temperatures, with an operating temperature range of up to 650 °C. These are easy to operate, reduce the cell fabrication cost by using the lower-cost materials, and have long-term durability. Among growing research fields, low-temperature SOFCs (LT-SOFCs) with high conversion efficiency are the need of the present era.

To work effectively at low temperatures, the development of critical components of the cell (cathodes, anodes, and electrolytes) and an in-depth understanding of materials science to obtain desired materials having exceptional properties, such as desired electrical conductivity, electrocatalytic activity, thermal stability, and chemical compatibility, are needs. In order to achieve the excellent performance of SOFC devices, there is a necessity for more investigations into versatile materials and their combinations to accomplish the materials requirements of SOFCs. Moreover, the development of SOFC devices for practical deployment is associated with tremendous technological challenges in energy material research, for example, material selection challenges in terms of cost, operating temperatures, and fabrication procedures.

As the core component of the SOFCs, the electrolyte plays an essential part in the performance of single cells since it decides the running temperature of the fuel cell and the related other components of the cell. Materials used as electrolytes in SOFCs could be an oxide ion conductor, a proton ion conductor, or a dual ion conductor. The characteristics of applied electrolyte materials decide the electrode reaction and performance of each cell configuration. In a SOFC, the primary role of a solid electrolyte is to conduct ions, either O^{2-} or H^+ (nature of the specific material), between the electrodes in order to avoid blocking electrons for internal conduction, driving the electrons to move through the outside external circuit to complete the overall electrochemical reaction. Materials used as electrolytes in SOFCs must have high ionic conductivity, chemically, thermally, and mechanically companionable with the adjoining cell components, highly dense microstructure, and low electronic conductivity to avoid internal short-circuits during the electrochemical reaction^[4-6].

In the last few decades, SOFC electrolyte materials have received significant attention from materials researchers and scientists in order to achieve good SOFC performance. Despite the rigorous necessity for electrolyte materials, the practical application of limited ionic conducting electrolyte materials has been a challenge. Various ionic conductors have been explored as electrolyte materials^[7-10], such as commonly used doped $CeO_2/Bi_2O_3/ZrO_2$ and $LaGaO_3$ -based perovskite oxide and newly developed $Ca_{12}Al_{14}O_{33}$ ^[8], $Ln_{10}(SiO_4)_6O_3$ [$Ln = La, Nd, Gadolinium (Gd), Samarium (Sm), and Dy$]^[9], $Na_{0.5}Bi_{0.5}TiO_3$ (NBT) and $La_2Mo_2O_9$ -based fast oxide ion conductors^[10]. Among these materials, oxygen (O_2) ionic conductors of the acceptor-doped ceria, yttrium stabilized zirconia, doped $LaGaO_3$ -based oxides, and proton conducting materials of barium zirconate and barium cerate have been the selected for SOFCs industrial and academic utilization. Yttrium-stabilized zirconia (YSZ) is the most common choice due to its high ionic conduction property at elevated operating temperatures (≥ 700 °C) and its capability to work effectively across a wide range of oxygen partial pressure. Still, for low-temperature operations, its ionic conductivity is not sufficient. The currently extensively implemented electrolyte materials, such as acceptor doped ceria and doped $LaGaO_3$ -based fast ionic conductor oxide, always undergo fundamental problems, such as the short circuit inside the system due to reduction in Ce^{4+} to Ce^{3+} and extreme chemical reactivity with the other common electrode materials for $LaGaO_3$ -based electrolyte materials. Other recently developed electrolytes, such as rare-earth-doped ortho-niobates and tantalates^[11], NBT^[12] and $Sr_{1-x}Na_xSiO_{3-0.5x}$ ^[13], still require more in-depth studies before being widely used akin to the above-stated electrolyte materials.

Worldwide, researchers and scientists put their efforts into reducing the operating temperature of SOFCs. The reduced operating temperature permits prolonged material and device lifespan and facilitates less investment cost. These are the two foremost concerns for product consumption in the market. The operating temperature reduction of electrolytes from a high-temperature range (800-1,000 °C) to a low to intermediate temperature range (300-700 °C) requires significantly less ohmic resistance. Two major approaches are implemented. In order to develop new electrolyte materials with high ionic conductivity, reducing the electrolyte thickness from its current micrometer scale to the nanometer scale is crucial. This reduction is necessary because, according to the ohmic laws, the ohmic resistance of electrolytes is directly related to the electrolyte thickness. Few interesting phenomena are observed when the thin film is reduced to in the range of nanometers, such as distinct improvement/diminution of the charge conduction transition such as electronic-to-ionic conduction or ionic-to-electronic conduction or proton charge conduction in the common oxide ion conductor in the range of low operating temperatures. For that reason, an alternative technique is dedicated to designing nanograin electrolytes with superionic charge conduction in a composite interface along the grain boundary (GB) and interface. Over the past few years, nanocomposite materials for advanced fuel cells have initiated an emergent Research & Development and global academia surge^[14]. Invented from this approach, fast ion conducting nanocomposite electrolyte

materials, such as core-shell and nanowire structural ceria-based nanocomposites, have exceptional ionic conductivity in temperatures over 300 °C in the order of 0.1 S cm^{-1} and a distinctive property of simultaneous O^{2-}/H^+ charge transfer has been developed for low temperatures in the range of 300-600 °C. Many investigations have proven that ceria-carbonate-based nanocomposite materials have the benefit of multi-ion charge conduction, and outstanding performances in LT-SOFCs enable them to be superior electrolytes for SOFC applications. The favorable characteristics of these proposed composite materials also provide them with possible applications in the safety of the environment, for example, the separation of CO_2 ^[15,16].

When protons pass through the electrolyte instead of oxide ions, the SOFC is also called protonic ceramic fuel cells (PCFCs). Compared to SOFCs, PCFCs may operate at reduced temperatures as diffusion of protons requires lower conducting activation energy (0.3-0.5 eV) than that of oxygen ions. Additionally, most proton-conductive ceramics have very high ion conductivity at a lower temperature than oxygen-conductive ceramics. Furthermore, PCFCs show relatively high efficiency and working performance in a low operating temperature range (600 °C or less). Another advantage of PCFCs is that the water, which is generated at cathodes as a by-product of the reaction, prevents fuel dilution in the anode.

Semiconductor membrane fuel cell: a novel concept of SOFCs

Recently, a major revolution in the development of SOFCs devices has been informed, i.e., single-layer/component or electrolyte-free fuel cell (SLFC or EFFC) and double layer fuel cell (DLFC) ^[17,18]. **Figure 1A** illustrates the conventional three-layer configuration of a SOFC with oxygen ion conducting electrolyte without electron passage. Here, the H_2 fuel is oxidized, and electrons are released at the anode side. While oxygen (O_2) is reduced to oxygen ions (O^{2-}) at the cathode side, which combine with electrons from external circuit to produce electricity. Interestingly, the double layer fuel cell (DLFC) device (as shown in **Figure 1B**) can perform even better than the electrolyte based SOFCs. As a result, DLFC demonstrates great potential for further advancement. The SCFCs on the other hand, as shown in **Figure 1C**, are consist of simply only one component having neither electrolyte membrane or electrodes (cathode and anode); however, they offer comparable, even superior performance than the traditional three-component fuel cells. The simple structure having a “three in one” system allows promoting their cost-effectiveness, which further enables them to exhibit a great potential to accelerate fuel cell commercialization. The vital part of SCFC or EFFC is the co-existence of semiconductors and ion conductors. These structures help in avoiding the internal short-circuiting problem and realize fuel cell nano-redox and processes at the nanoscale or at the particle level, as shown in **Figure 1D**.

Another significant area of research interest is the interfaces developed among semiconductor-ionic, semiconductor-insulator, semiconductor-semiconductor, or oxides, known as Semiconductor membrane/Semiconductor-ionic membrane fuel cells, which influences the variation in bandgap and charge conduction properties. The primary interest in these fuel cells is to lead to changes of ionic transport properties in the form of interfacial or surface electronic band and state changes. It has been discovered that these changes can be reached in different semiconductors and heterostructure composites of semiconductors can possess similar ionic conduction and fuel cell power. This points out that the ionic charge transport process may have a similar origin across various interfaces modified by energy bands. The role of electron band states and structures in composite interfaces of these materials is important as ion transportation is determined by the local electron charge density and the electric field along the interfaces of heterostructure composite oxide materials, as shown in **Figure 1E**. Recent literature articles reveal that semiconductor-ionic composite heterostructure materials drastically improve ionic conductivity, as earlier reported that a $\text{YSZ}/\text{SrTiO}_3$ composite mixture has exhibited an improved ionic conductivity value compared to YSZ ^[19].

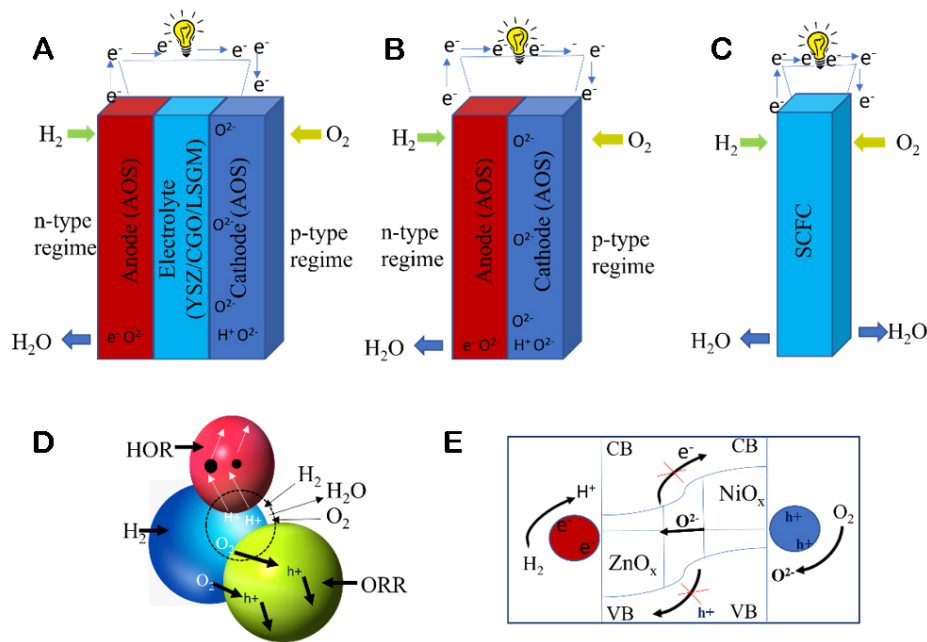


Figure 1. Schematic representation of different kinds of fuel cells: (A) conventional solid oxide fuel cells (SOFCs). (B) double-layer fuel cells (DLFCs), (C) single component fuel cells (SCFCs), (D) SCFC–nano redox fuel cells, (E) band alignment for SCFCs. Adapted and modified from Ref.^[32].

A new characteristic of fuel cell technology from semiconductor physics was first presented by Singh *et al.* in 2013^[20], where amphoteric oxide semiconductor cathodes and anodes separated by an ionic conducting electrolyte are renowned as *p*- and *n*-type regimes, respectively. The ion conducting electrolyte materials possess the same properties as intrinsic semiconductors, having a bandgap of a larger value; for example, the bandgap of YSZ is 5.79 eV^[21,22]. Meanwhile, the cathode and anode, placed in an oxidizing and reducing environment, respectively, are responsible for ORR and HOR and possess high hole/electronic conductivity^[23]. Therefore, extrinsic semiconductors having low bandgaps are required to enable sufficient *p*-type and *n*-type charge conduction, as shown in Figure 1D. A common example is the typical family of perovskite oxide electrode materials having mixed ionic and electronic conductivity^[24].

In order to summarize by using the semiconductor physics aspect, the SOFCs can correspond to a three-layer *p-i-n* semiconductor device by applying a corresponding *p*-type cathode, intrinsic semiconductor-type electrolyte, and *n*-type anode^[25-27]. Furthermore, a *p-n* two-component/layer device, i.e., DLFC, as represented in Figure 1B, similar to a *p-n* heterojunction device, is designed when the middle layer of electrolyte (*i*-type) is removed. The *p-n* junctions consisting of bulk heterojunction *p-n* type materials, i.e., Single-Layer Fuel Cells (SLFC) having ionic conductors mixed with *n*- and *p*-type semiconductors, which have been widely reported for the formation of electric field barriers to avert the further movement of the hole from *p* to *n* layer and electron transportation from *n*-type to *p*-type layers until the bending of the band is accomplished^[17,28,29]. New designing approaches of semiconductor heterojunction-based fuel cells using important aspects of energy band/alignment and built-in electric field (BIEF) create barriers for the electron transport while supporting superionic charge transport along the interfaces and afterward improve the performances of the device in working conditions^[30-32].

Based on rigorous investigations and developments of semiconductor membrane fuel cell (SMFC) materials and device technologies, this review will cover the principal understandings, historical development, and

achievements in the last few decades. Its further objectives are to afford a novel method and approach by presenting the semiconductor energy band and BIEF theories as a common technical foundation to design Semiconductor Ionics to develop next-new-generation superionic materials with self-field driving ionic transport at low temperatures of 300-500 °C.

SEMICONDUCTOR ELECTROLYTE MATERIALS FOR SOFC

From material physics aspects, all currently used materials for SOFC/PCFC electrolytes and electrodes, such as perovskite oxide, fluorite, spinel, layered structured material, *etc.*, are semiconductor materials. These used materials are either wide bandgap semiconductors for ionic conducting electrolytes or narrow bands for mixed or triple charge conducting electrodes. Using the physical and semiconductor properties of materials, we are able to deepen the understanding of the material's nature, improve or develop new functions with performance, and understand the fundamental science of the device function^[11,12,32-34]. In this section, we will discuss the structural aspect of the materials that have been extensively studied by the researchers.

Fluorite

The fluorite oxides with a general formula AO_2 (A = mainly large tetravalent cations such as Ce, U, *etc.*) are known to be good oxygen ion (O^{2-}) conductors. This structural configuration results in an open structure consisting of interstitial octahedral voids, which helps tolerate doping on a large scale and endorses ionic conduction. One example is ZrO_2 , where Zr^{4+} is partially substituted by a larger cation Y^{3+} , resulting in yttria-stabilized zirconia (YSZ) composition with high ionic conductivity due to the creation of oxygen vacancy for the sake of charge neutrality of the composition, as shown in [Figure 2A](#)^[35]. Another popular example is ceria, which has a fluorite structure and Ce^{4+} mainly partially replaced by lower valence Gd^{3+} or Sm^{3+} to create gadolinium-doped ceria (GDC) and samarium-doped ceria (SDC), as illustrated in [Figure 2B](#)^[36]. The compositions have been used extensively as electrolytes in SOFCs. In recent years, many novel research developments have reported that fluorite can be used as a proton conductor, which is an interesting topic and will be further discussed in the following chapter.

From the semiconductor aspect, fluorite-structured oxides are wide bandgap materials with a bandgap larger than 3.0 eV. Therefore, these materials naturally show very low or neglectable electronic conduction compared to their ionic (O^{2-} or H^+) one, thus, good for electrolyte applications. Moreover, recent developments have shown that the ceria and zirconia fluorite oxides also possess proton conductivity, which is getting more interesting in the new development of LT-SOFCs. We will start a new session in the next chapter "Proton conducting electrolyte".

Perovskite oxide

The perovskite oxides are technologically important materials having applications in different fields due to their unique properties^[37-39]. The general formula of perovskite oxide is ABO_3 , where A-site cations are alkaline, alkaline earth, and lanthanide ions, whereas B-site cations are mainly transition metal ions^[40]. Although the ideal ABO_3 structure has a cubic phase with a $Pm\bar{3}m$ space group, other phases, such as orthorhombic and tetragonal, are also found^[41]. In the cubic unit cell, the B-site cation sits at the center of the cube, forming BO_6 octahedra with oxygen atoms residing at the center of the faces, while the A-site cation sits on the corner of the cube. The structure can also be viewed in an alternative way, as shown in [Figure 3A-C](#), emphasizing the formation of BO_6 octahedra in the unit cell. In real situations, most of the perovskite oxides show non-cubic phases, i.e., orthorhombic, tetragonal, and rhombohedral phases, due to distortion in BO_6 octahedra, which is mainly caused by the large size of A-site cations. The Goldschmidt tolerance factor (t), introduced by Goldschmidt by the following equation (Equation 1), actually gives an idea of the distortion^[42].

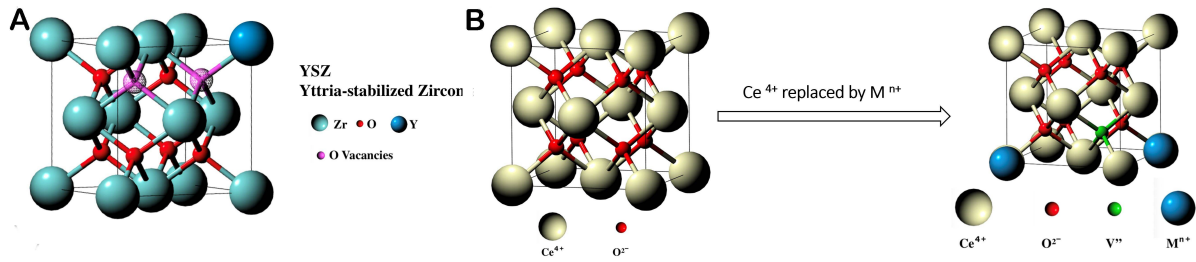


Figure 2. (A) Yttria-stabilized zirconia (YSZ) is a cubic crystal structure of zirconium dioxide with the addition of yttrium oxide. (B) Ceria has a fluorite structure and is mainly partially replaced by lower-valence Mⁿ⁺ (Gd³⁺ or Sm³⁺) to create gadolinium/samarium-doped ceria (GDC)^[36].

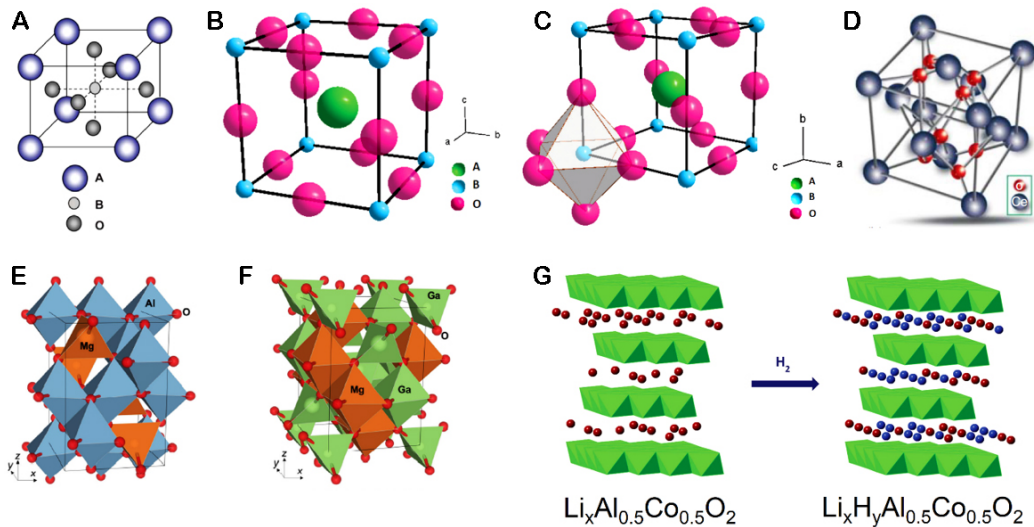


Figure 3. ABO₃ perovskite structure: (A) B-site cation at the center of the unit cell, (B) A-site cation at the center of the unit cell, (C) emphasizes the BO₆ octahedra formation and (D) unit cell of fluorite CeO₂. Reproduced under the terms of the CC BY 3.0 License Copyright 2020, Book Chapter Published by Intechopen^[51], (E) MgAl₂O₄ normal spinel structure, (F) MgGa₂O₄ inverse spinel structure. Unit cells, along with different coordination environments, are reproduced under the terms of the CC BY 4.0 License Copyright 2020, Published by Springer Nature^[53]. (G) Proton insertion in layered Li compound where Li⁺ is the red-colored sphere, and H⁺ is the blue-colored sphere. Reproduced with permission^[54] copyright 2014 John Wiley and Sons.

$$t = \frac{r_A + r_O}{\sqrt{2}(r_B + r_O)} \quad (1)$$

where r_A , r_B , and r_O are the ionic radii for A, B, and O, respectively.

For cubic structures, the t value resides between 0.9-1, whereas if it is greater than 1, then a hexagonal or tetragonal structure can be formed. An orthorhombic or rhombohedral structure can be formed when the value is between 0.71 and 0.9. The properties of perovskite, such as oxygen ion vacancy, structural defects, ionic or mixed ionic and electronic conductivity, oxygen exchange kinetics, creation of redox couples, and stability, can be tailored by introducing more than one cation both at A- and B-sites of the structure^[43]. The structural flexibility allows perovskite oxide for various applications in SOFC/PCFC, e.g., LaGaO₃-based electrolytes as O²⁻ conducting electrolytes^[44] and BaZrO₃ and BaCeO₃-based perovskites for H⁺ conducting electrolytes used for PCFCs^[45]; more commonly, mixed electronic and ionic or triple charge (O²⁻/H⁺/e⁻) conducting perovskites have been widely used as electrodes, mostly for cathodes^[46-48], but also some for anodes^[49-50].

Spinel

Basic ABO_3 perovskite-type structures typically feature B-site cations at the center of the unit cell and A-site cations at the center of the unit cell, as shown in Figure 3A and B. Further, Figure 3C emphasizes the BO_6 octahedra formation. The unit cell consists of cations sitting at the corner and center of faces in the cubic lattice while the oxygen atoms occupy the tetrahedral sites, as demonstrated in Figure 3D^[51]. Spinel is known for their application in the energy storage, but recently, they are being explored for other applications because of their encouraging catalytic properties. The normal spinel is generally represented by the formula $[A]^t[B_2]^oO_4$ (t and o represent the tetrahedral and octahedral sites, respectively). The structure is a face-centered cubic lattice where A-site atoms occupied 18 tetrahedral voids and B-site atoms occupied 12 octahedral voids, making them tetrahedrally and octahedrally coordinated, respectively. On the other hand, the structure of inverse spinels is the opposite, where B-site atoms sit on the tetrahedral sites and both A and B-site atoms are in the octahedral sites^[52,53]. The structures of normal spinels ($MgAl_2O_4$) and inverse spinels ($MgGa_2O_4$) are shown in Figure 3E and F.

Other structures

Apart from the abovementioned oxide materials, there are other structures that have been recently used as electrolytes in SOFCs. Lithium-based layered oxides are now investigated as potential electrolyte materials^[54]. At first, Sebastian *et al.* showed possible modification of material from lithium-ion to proton conductors by replacing Li^+ with H^+ in lithium-ion conductors using reversible ion exchange methods^[55]. This work opens up new possibilities for layered structured materials^[54,55]. Lan *et al.* showed that hydrogen (H_2)-inserted structure, $Li_xH_yAl_{0.5}Co_{0.5}O_2$, can be made from a layered lithium-based oxide material, $Li_xAl_{0.5}Co_{0.5}O_2$, at high temperature in a hydrogen atmosphere^[54]. The proton insertion process is shown in Figure 3G. The resultant material showed an enhanced value of proton ion conductivity.

Moreover, many researchers have applied the heterostructure concept to further improve the performance of the electrolytes. When a composite containing *p*- and *n*-type semiconductors is formed, electrons will move from *n*-type to *p*-type during experimental conditions, giving an opportunity to create superionic conductors. Composites containing semiconductors and ionic conductors have also been explored extensively, resulting in improved ionic conductivity several times^[19]. The concept will be discussed in detail in the upcoming sections.

APPLICATION OF SEMICONDUCTORS IN SOFC

One of the major issues in the SOFC field is electrolytes' ionic conductivity at low temperatures. Researchers studied different kinds of materials as electrolytes to address the issue. Apart from new materials, other routes, such as thin film formation, thickness reduction, and layered electrolyte generation, have been considered in the last few decades. Although the improvement is significant, it falls short of meeting the standards required for commercialization. Recently, semiconductor materials have been considered for studies to address the issue. Apart from single-phase materials, heterostructure semiconductors are also considered. In this section, we will discuss in detail the work that has been done with these materials as electrolytes.

Oxygen ion conducting electrolyte

A significant amount of work has been done for decades on oxygen ion conducting electrolytes for SOFCs. In this subsection, we will discuss the compositions that have been studied extensively.

YSZ is the most studied electrolyte composition to date, mainly due to its high ionic conductivity. Pure ZrO_2 shows different phases depending upon the temperature, such as monoclinic at room temperature, tetragonal above 1,100 °C, and cubic fluorite above 2,370 °C, along with low oxide ion conductivity because of limited oxygen ion vacancies. It is observed that doping of Y^{3+} in the ZrO_2 structure results in stabilization of the fluorite phase at room temperature along with enhancement of oxygen ion conductivity by creating more vacancies. YSZ [8 mol% YSZ (8YSZ)] shows high ionic conductivity of 0.14 S cm^{-1} at 1,000 °C. This high temperature is not suitable for ultimate application purposes due to cell degradation^[56]. Therefore, the main challenge for YSZ electrolytes is to reduce their operational temperatures without compromising their ionic conductivity. So, the researchers have tried to lower the temperature by applying various innovative modification techniques such as densification, sintering modification, and thin layer formation. Thin-film formation is found to be very effective in this regard.

Esposito *et al.* made thin-film YSZ electrolytes by using an inkjet printer that contains YSZ nanoparticles, which yielded a high-power density of 1.5 W cm^{-2} at 800 °C^[57]. Park *et al.* used the atomic layer deposition (ALD) technique to fabricate thin-film YSZ electrolytes, resulting in higher conductivity and astonishing fuel-cell performance with an open-circuit voltage (OCV) near 1 V at 1,000 °C^[58]. Apart from thin films, different unique types of modifications have also been applied by various groups. For example, Lu *et al.* reported lower area-specific resistance (ASR) of YSZ electrolytes by the introduction of $\text{Ca}_3\text{Co}_2\text{O}_6$ and $\text{Sm}_{0.2}\text{Ce}_{0.8}\text{O}_{1.9}$ as interlayers^[59]. Lee *et al.* achieved several benefits, such as sintering temperature drop, grain growth, and eutectic liquid creation, by introducing Li as a dopant in YSZ^[60]. Xu *et al.* prepared a composite containing YSZ and mineral CuFe-oxide minerals, which shows high ionic conductivity and power density^[61]. Liu *et al.* prepared the electrolyte by a combination of conventional YSZ and YSZ nanowires synthesized by electrospinning techniques, resulting in ionic conductivity of 0.01 S cm^{-1} at 375 °C, which is 290 times better than the bulk YSZ^[62]. Han *et al.* observed that the effect of grain size reduction is more prominent in the low and intermediate temperature range (up to 800 °C)^[63]. This is due to the enhancement of thickness of the intergranular region with grain size reduction, which mainly contains a maximum of three atom layers. Because of this, oxygen ion conduction is not interrupted due to segregation or impurity. So, the mixed grain and GB give an easy road for ionic movement, as shown in Figure 4A.

Yamamoto *et al.* show the trend of ionic conductivity with lanthanide doping in ZrO_2 shown in Figure 4B^[64]. It has been observed that Sc-doped ZrO_2 establishes the greatest conductivity of 0.3 S cm^{-1} at 1,000 °C. Therefore, much focus has been given to the scandia-stabilized zirconia (ScSZ) composition. The introduction of Sc_2O_3 in zirconium increases the oxygen ion vacancy, resulting in fast ionic movement and less ohmic resistance. The optimized Sc_2O_3 concentration is an important factor for structure stabilization and high performance. It has been observed that doping of 5-9 mol% Sc_2O_3 generates the cubic phase while 10-15 mol% results in rhombohedral phase structures.

Another fluorite-structured oxide, CeO_2 , has enticed the concentration of the research community because of its potential application as an electrolyte for low-temperature fuel cells. Anirban *et al.* described that ceria is basically an insulator; the partial substitution of acceptor cations into the ceria lattice introduces oxygen vacancy defects that influence the ionic conductivity at relatively low operating temperatures^[65]. The ionic conductivity of ceria can be significantly enhanced by doping rare earth cations, such as $\text{Ce}_{0.8}\text{RE}_{0.2}\text{O}_{1.9}$ (RE = Er, Ho, Gd, Eu, Sm, Nd, and La), which create defects associated with the structure. The variation of ionic radii of the dopant cations plays an important role in the value of ionic conductivity and activation energy, which can be explained with the help of existence of defect associates. Among other rare earth-doped ceria electrolytes, the Gd^{3+} -doped ceria shows the highest conductivity and the lowest activation energies. Although significant progress has been achieved with this material, some critical challenges

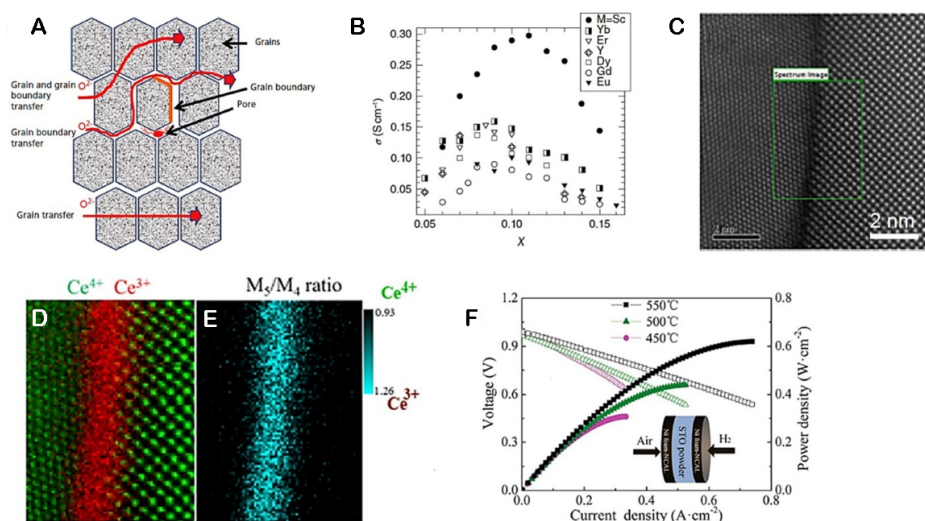


Figure 4. (A) Schematic representation of large grain and grain boundary area, along with routes for ionic conduction. Reproduced with permission^[63] Copyright 2007 Elsevier, (B) ionic conductivity comparison of various compositions [Ln₂O₃ (Ln = lanthanide)-doped ZrO₂] at 1,000 °C. Reprinted with permission^[64] Copyright 2000 Elsevier, (C) HAADF image of grain boundary of CeO_{2-δ}@CeO₂ core-shell, (D) mapping of Ce at the interface (E) ratio of Ce⁴⁺/Ce³⁺ at the interface. Reprinted under the terms of the CC BY 4.0 License Copyright 2019, Published by Springer Nature^[67]. (F) Voltage-current density-power density plot SrTiO₃ at different temperatures (450, 500, 550 °C). Reprinted from Ref.^[68] with permission from the Royal Society of Chemistry, 2019.

include reducing the electrolyte by hydrogen, which reduces OCV and power density, and enhancing electronic conduction on the transition from micro to nanometer scale remains as bottlenecks for its practical application. Doped ceria compositions are suitable for low-temperature applications (below 600 °C) because it is observed that OCV and the efficiency of SDC lower with an increase in temperature. High-temperature sintering (above 1,600 °C) for densification is another issue for ceria-based electrolyte fabrication. Therefore, novel synthesis techniques, such as solvothermal, co-precipitation sol-gel, *etc.*, have been adopted to create ceria nanomaterials that reduce the required sintering temperature. Apart from synthesis techniques, sintering aid has also been applied. Singh *et al.* revealed that co-doping approaches are useful for getting better conductivity of electrolytes simply at an intermediate temperature range and at an optimum concentration of dopants^[66]. Wang *et al.* conducted a study where they deliberately introduced various surface defects and altered the electrical properties of CeO₂ in order to examine the relationship between conductivity and surface states^[67]. The CeO_{2-δ}@CeO₂ core-shell heterostructure was clearly revealed by using scanning transmission electron microscopy (STEM) and electron energy-loss spectroscopy (EELS), as demonstrated in Figure 4C-E. These techniques conclusively established that the surface buried layer, spanning a few nanometers, consisted of Ce³⁺ on ceria particles.

Apart from fluorite structures, perovskite oxides have also been studied as electrolytes. Doped lanthanum gallates show promising results. Ishihara *et al.* found that La_{1-x}Sr_xGa_{1-y}Mg_yO_{3-δ} (LSGM) shows very good oxygen ion conductivity (~0.14 S cm⁻¹ at 800 °C), which is better than stabilized zirconia along with stability^[44]. Although LSGM shows potential, it faces several challenges such as phase purity, internal diffusion, and mechanical strength up to the present. Chen *et al.* prepared SrTiO₃ perovskites as an electrolyte, which showed superior ionic conductivity of 0.24 S cm⁻¹ and a high-power density of 620 mW cm⁻² at 550 °C, as shown in Figure 4F^[68]. Although many potential candidates are found, much more research and introduction of new concepts are required to get the ultimate composition for practical use.

Proton conducting electrolyte

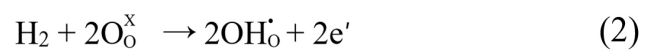
Proton conducting perovskite electrolyte

In 1981, firstly, Iwahara *et al.* observed the proton conduction in a few perovskite-structured oxide electrolytes such as SrCeO₃-based and BaCeO₃-based oxides^[69]. These materials were employed as electrolytes for hydrogen generation from water electrolysis at high temperatures. At high temperatures, the proton ion conduction is similar to oxide ionic conduction due to the small ionic radius and reduced ionic mass. Still, because of low activation energy, its value is higher at a temperature below 600 °C. Furthermore, numerous efforts have been made to develop a superior proton ion conductor and corresponding electrode materials for great performance and stability in working conditions. It has been reported earlier that the commonly used perovskite-structured proton conductor oxide, BaCeO₃, possesses excellent proton conductivity but undergoes poor chemical stability by being easily poisoned by CO₂ and steam in the air. Although BaZrO₃-based oxide showed notable stability in working conditions, it still suffers from poor sinterability and low proton ion conduction because of trapping of proton at the GB. There is constantly a trade-off effect between chemical stability and proton conductivity. In 2006, for the first time, Tao and Irvine employed ZnO in 1 wt% as sinter aids to enhance the sintering property of Ba(Zr,Y)O₃. Significant shrinkage of up to 15% can be detected when the temperature is raised from room temperature to 1,200 °C, whereas the pristine sample exhibits only 2% shrinkage^[70]. At that time, over the literature values, the ZnO-added sample exhibited the highest proton conductivity. Later, it was reported by Zuo *et al.* that the Y and Zr co-doped BaCeO₃ (BZCY) sample exhibits better as a proton conductor-based electrolyte for SOFC applications at low temperatures^[71]. Introducing Zr as a dopant enhances the poison resistance for steam and CO₂, whereas the addition of Y carries extra oxygen vacancies, promoting proton ionic conduction.

Proton conducting fluorite electrolyte

GDC has a fluoride structure, which has been extensively studied as an O²⁻ conducting electrolyte in SOFC applications. However, in recent years, new developments in fluorite proton conducting properties have gained a lot of importance^[72-76]. Zhao *et al.* provided evidence of introduction of surface reactive oxygen species to the CeO₂ substrate through DFT calculations^[72]. They found that desorption of adsorbed hydrogen (H⁺) intermediates can be promoted. Scherrer *et al.* reported YSZ thin films that have proton conduction via chemisorbed water at the inner surface in addition to oxygen ion conductivity, while above 400 °C, it turns to oxygen ion conduction^[73]. Shirpour *et al.* found doped CeO₂ exhibited higher conductivity than pure CeO₂^[74]. When the wet atmosphere was applied, a slight improvement in GB conductivity could be observed. Another research mentioned a transference of adsorbed water layers from an “ice-like” to a “water-like” structure for ceria fluoride materials, along with the shift in proton conduction mode^[75]. However, there was no clear understanding of why the proton mobility at the GB of a nanocrystalline material might be so high compared to the bulk. In this research, protonic surface conduction has been proposed with two series of connected processes that together compose a parallel rail to the bulk and GB conduction of oxide ions. These are intra-grain transport along the single grain’s surface and inter-grain transport conduction across the intersection between two adjacent grains, where the latter is highly resistive at low relative humidity^[75,76].

However, it should be noted that all these reports concerning water or humidity as a basic need when intra-grain transport occurs based on water contents, but the water cannot sustain at high temperatures, say 500 °C, then water molecular-associated proton conduction rapidly disappears. In this circumstance, some research could be carried out with dry H₂ to identify proton conduction directly under fuel cell operations. In this case, protons are produced through the following defect formation:



Recent research indicates protons can conduct along a pathway at the interface of the CeO₂ core and CeO_{2-δ} shell^[77]. The maximum power density of 697 mW cm⁻² was achieved for CeO₂/CeO_{2-δ} fuel cell configurations^[77]. It has demonstrated that proton conductivity can sustain at high temperatures, e.g., above 500 °C. In fact, a number of ceria-based materials have been reported at 400-600 °C region with high proton conductivity and successful fuel cell applications^[78,79]. For example, Li *et al.* reported some proton conducting CeO₂ nanocubes^[78] (as shown in Figure 5), and Paydar *et al.* reported surficial proton conducting CeO₂ nanosheets, as shown in Figure 6A^[79]. Figure 6 summarizes proton conducting ceria with various morphologies such as CeO₂ nanosheets and CeO₂ nanoparticles [Figure 6B]. Between 300-600 °C and below 200 °C, there has been numerous ceria, and zirconia-based fluorites have been reported for proton conductivity.

Mixed ion conducting electrolyte

Concern about the low-temperature operation of SOFCs has been raising emergent interest in recent years. Recent progress in perovskite oxide phases has led to the development of H⁺/O²⁻/e⁻ triple-conducting electrode BaCo_{0.4}Fe_{0.4}Zr_{0.1}Y_{0.1}O_{3-δ} (BCFZY) for the low-temperature operation of fuel cells. Xia *et al.* have developed a high ionic conductor, BCFZY electrolytes, and fabricated a BCFZY -ZnO composite *p-n* heterojunction-structured material in order to suppress its electronic conduction^[30]. Through this methodology, it has been established that BCFZY could be used in the operation of fuel cells with good performance as electrolytes, attaining extraordinary ionic conductivity, durability, and cell working performance. The energy band alignment mechanism can explain the electronic conductivity suppression and improvement of oxide ion conductivity in the *p-n* heterostructure. The research outcomes reveal that BCFZY is a promising electrode and an excellent electrolyte.

New electrolytes based on semiconductors

In addition to the abovementioned commonly reported and typically used electrolyte materials, there are various newly developed electrolyte materials for SOFCs, such as oxygen ionic conducting apatite structure Ln₁₀(SiO₄)₆O₃ (Ln = La, Nd, Sm, Gd, and Dy). Although it is generally believed that silicate-containing compositions are not as beneficial as the oxygen ion conductor of electrolytes, the conductivity of materials could still reach the value of 2.3 × 10⁻⁴ S cm⁻¹ at 500 °C^[9]. The presence of a higher oxygen-containing unit formula and improved oxide ionic conductivity propose the significant role of interstitial oxygen in charge conduction mechanisms. Lacorre *et al.* suggested the La₂Mo₂O₉-based oxide ionic conductor possesses a phase transition at a temperature of around 580 °C^[10]. Furthermore, the oxide ion conductivity continued to increase for more than two orders of magnitude as the conductivity value reached 6 × 10⁻² S cm⁻¹ at 800 °C, which is comparable to YSZ. In 2004, it was first reported by Li *et al.* that the classic lead-free piezoelectric material, NBT, unexpectedly showed excellent oxide ionic conductivity^[12]. Via Mg doping, the value of ionic conductivity could be improved to 1 × 10⁻² S cm⁻¹ at a temperature of 600 °C, and the value of conductivity possesses a higher value than that of GDC at a temperature below 500 °C. The low sintering temperature, excellent ionic conductivity, and less expensive precursor materials recommend NBT as a potential rare earth metal-free electrolyte for application in SOFCs, particularly for low working temperature ranges. Goodenough first reported that the sodium/potassium-modified Sr (Si, Ge)O₃ has an excellent ionic conductivity of 1 × 10⁻² S cm⁻² at the temperature of 625 °C. The doping of potassium/sodium at the strontium lattice site induces the generation of oxygen vacancy, which could not be either accommodated through the sharing of the corner with a neighboring (Si/Ge)₃O₉ unit or accommodated through a distortion that would result in a mobile oxide ion at the interstitial site, leading to enhancement in oxide ionic conductivity, which makes them competitive ionic conductor for IT-SOFCs having low-cost potentiality^[13].

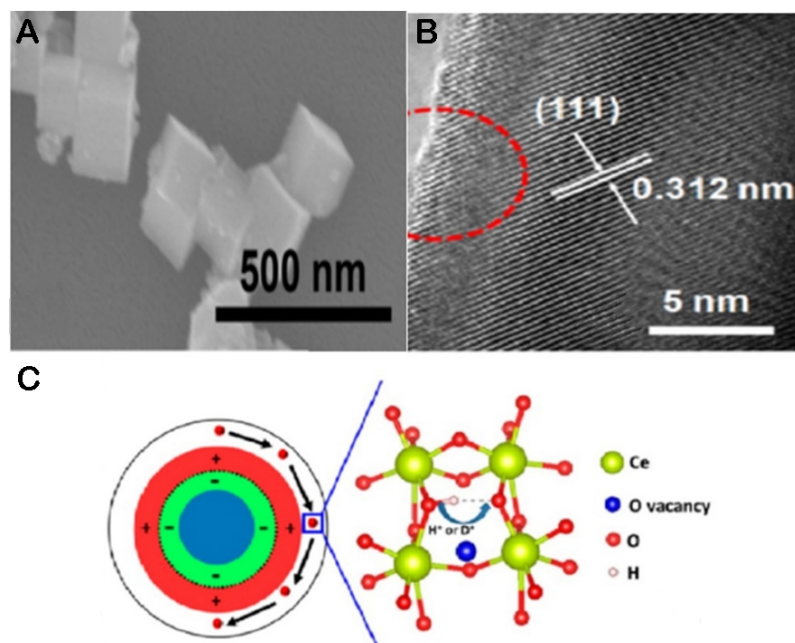


Figure 5. Different CeO₂ morphologies (A) Nanocube. Copyright 2018, International Journal of Hydrogen Energy^[78]; (B) core-shell and (C) proton conduction in the shell layer^[78].

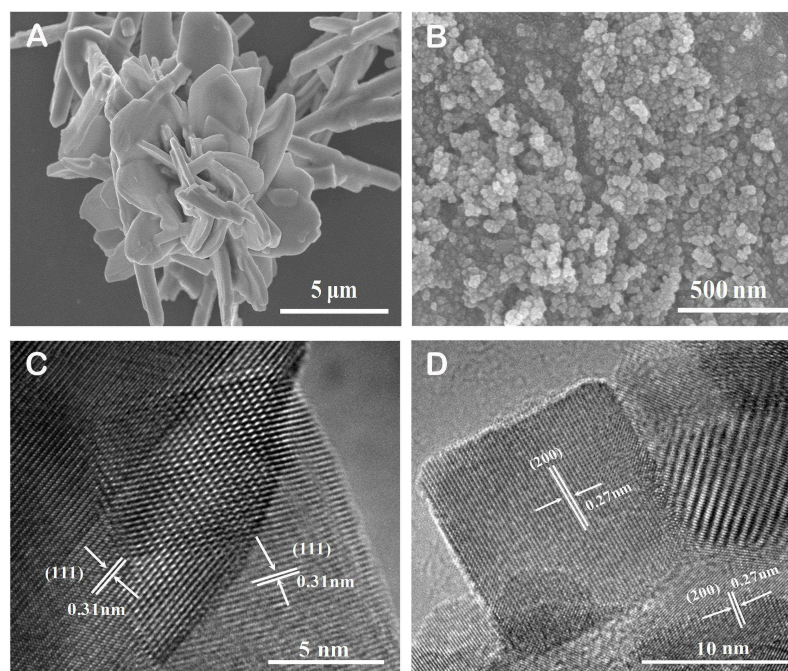


Figure 6. SEM images of (A) CeO₂ nanosheets, (B) CeO₂ nanoparticles, HRTEM images of (C) CeO₂ nanosheets, (D) CeO₂ nanoparticles. Copyright 2023, Ceramics International^[79].

Heterostructure composite materials

Ceria/carbonate composite materials

Different categories of electrolyte materials, such as zirconia-doped, bismuth-doped, lanthanum gallate-doped, and ceria-doped materials, are well documented in the literature. Among these, ceria-doped

materials have shown considerable interest as novel electrolyte materials for LT-SOFCs^[73,75,76,80,81]. Since then, enormous progress has been made in this area to understand and improve the properties of ceria-based materials. For example, structural doping of ceria Ce^{4+} by lower valent cations such as Sm^{3+} or Gd^{3+} . By doing so, SDC and GDC have achieved a higher ionic conductivity of 0.1 S cm^{-1} at $800 \text{ }^\circ\text{C}$ compared to YSZ (at $1,000 \text{ }^\circ\text{C}$). However, in reducing conditions, ceria-doped electrolytes show significant electronic conduction due to the reduction of Ce^{4+} to Ce^{3+} , which leads to significant electrochemical leakage and micro-cracking due to a significant change in volume. These shortcomings pose significant challenges to the stable operation of doped ceria electrolytes^[81].

An alternative approach to improve this shortcoming of the ceria-based electrolytes is to introduce the second-phase materials, e.g., carbonates and semiconductors, to form a ceria-based heterostructure (CHC) composites, which showed stable operation at reducing atmosphere^[31,82]. Heterostructure technologies have been regarded as promising methods in the development of electrolytes with high ionic conductivity for LT-SOFCs. Also, in reducing conditions, CHC composites with a core-shell structure, where ceria constitutes a core and with a carbonate shell, could overcome the anodic reduction of doped ceria electrolytes. Additionally, the shell can release the internal stress to avoid micro-cracking.

Several reports on stable operation of ceria-carbonate systems from 1500 h to above 6000 h have been reported in the literature^[71,83]. Further, ceria-carbonate CHC materials show multi- $(\text{H}^+/\text{O}^{2-}/\text{CO}_3^{2-})$ or hybrid-ion $(\text{H}^+/\text{O}^{2-})$ conduction as electrolytes, which showed high ionic conductivity with excellent LT-SOFC performances^[81,84] and resulted in attracting new research and development activities. Several reviews have been published in the literature, especially to explain the superionic conduction in the ceria-carbonate heterostructure composite materials based on multi-ionic conduction at the interface^[14,85,86].

Further, the latest developments have demonstrated promising new materials for ceria-semiconductor CHCs^[32]. In 2011, Zhu *et al.* discovered homogenous single layers by mixing doped ceria, ionic conductors, e.g., SDC or GDC, and semiconductors to integrate all functions from fuel cell anodes, electrolytes, and cathodes into one-layer components^[18]. These Semiconductor-Ionic single layers can be seen as ceria-semiconductor heterostructure composite systems. In the last decades, lots of studies have been carried out to fully understand the internal conduction mechanism of ceria-semiconductor heterostructure composites from the micro-level^[29]. The ceria-carbonate or semiconductor heterostructure composites are showing new promising functionalities based on heterostructure composite materials with wide energy applications^[32]. A more comprehensive description of ceria or ionic/semiconductor composite materials is described in section “Semiconductor-ionic composite materials”.

Semiconductor-ionic composite materials

Semiconductor heterostructures incorporated with one ionic phase and another semiconductor phase can provide better performance than conventional electrolytes (e.g., single-phase electrolytes). Semiconductor-ionic heterostructure composite materials can achieve higher ionic conductivity and subsequently increase the triple-phase boundary for electrode reactions^[87-89]. For example, when combining the semiconductor phase, *p*-type LiZnO, with the ionic phase of doped ceria (*n*-type under fuel electrode conditions), we observe superionic conductivity ($> 0.1 \text{ S cm}^{-1}$ over $300 \text{ }^\circ\text{C}$) and excellent electrolytic performance ($400\text{-}630 \text{ mW cm}^{-2}$) for LT SOFCs.

Basically, we combined a *p*-type and *n*-type semiconductor, which resulted in a *p-n* junction. Here, separation of charges (electrons/holes), along with accelerated ion transport, could be realized along the heterojunction or semiconductor interface. Thus, such *p-n* heterojunction composite materials can be potential materials for the electrolyte without electronic leakage issues^[30,90].

Lots of new materials on Semiconductor-ionic heterostructure electrolyte composite materials have been reported in the literature, which show high ionic conductivity and excellent fuel cell electrochemical performances^[54,91,92]. The semiconductor-ionic approach may provide a new method to realize the challenge for current SOFCs caused by the poor ionic conductivity of electrolytes at a low-temperature regime. Several reports suggested that ceria-semiconductor CHC composites show a substantial increase in ionic conductivity enhancement (two or more orders of the magnitudes) between a semiconductor (e.g., perovskites, such as SrTiO₃) and an ionic electrolyte (such as YSZ/SDC/GDC)^[19,93-95]. However, the presence of strong electronic conduction in such heterostructure materials can cause serious OCV and power losses, and their fuel cell performance in SOFCs remains a question.

Semiconductor-ionic heterostructure materials have created new-type fuel cell devices, e.g., single-layer EFFC^[18,96-98] and semiconductor-ionic fuel cells (SIFC)^[30,31,99,100]. Further, the fuel cell research group led by Zhu *et al.* demonstrated various semiconductor physical heterojunctions, e.g., bulk-pn-heterojunction^[29], Schottky junction (S)^[101], and band alignment^[28], to understand the device working mechanism and principle.

Recently, there has been significant publication of work claiming that such semiconductor-ionic heterostructure composites, if used as electrolyte materials, result in high performance^[52,100]. Also, studies have been conducted to investigate fundamental issues of charge separation and transport^[28,31]. For example, one such investigation involved employing the semiconductor-ionic material La_{0.6}Sr_{0.4}Co_{0.2}Fe_{0.8}O_{3-δ} (LSCF) and the ion conductor, Sm³⁺ and Ca²⁺ co-doped ceria, as a form of the semiconductor-ionic composite material. In this study, a device was constructed by sandwiching the LSCF-SCDC between two layers of semiconducting oxide Ni_{0.8}Co_{0.15}Al_{0.05}Li-oxide (NCAL) thin films. The authors claimed the working mechanism is similar to a fuel cell using a pure ion conducting electrolyte added by p and n-blocking layers to prevent electrons from short-circuit^[28,31]. Semiconductor-ionic heterostructure composite materials-based fuel cells may suggest an alternative promising approach to developing next-generation SOFCs.

MECHANISM OF IONIC TRANSPORT IN ELECTROLYTES

Structural doping and bulk conduction

In a SOFC, the primary role of solid electrolytes is to conduct ions, either O²⁻ or H⁺ (nature of the specific material), between the electrodes in order to avoid blocking electrons' internal conduction, driving the electrons to move through the outside external circuit to complete the overall electrochemical reaction. Materials used as electrolytes in SOFCs must have high oxygen ion conductivity, chemically, thermally, and mechanically companionable with the adjoining cell components, highly dense microstructure, and low electronic conductivity to avoid internal short-circuits during electrochemical reactions^[4,6,102]. In the last few decades, SOFC electrolyte materials have received great attention from researchers and scientists in order to achieve good SOFC performance^[85,103]. Therefore, a wide variety of compounds have been investigated as suitable candidates for electrolyte materials for SOFCs. The major research work has been focused mainly on four categories of electrolyte materials, viz. YSZ, GDC/SDC, doped bismuth, and doped lanthanum gallate^[103-105]. In order to improve the ionic conductivity of these systems, single or multiple dopants in each of these four systems of materials have been further sub-categorized.

The ionic conductivity of electrolytes, such as doped ceria, originates through ion movement in lattice under the effect of an electric field. The electrical conductivity σ can be expressed as:

$$\sigma = n * e * \mu \quad (3)$$

Where σ , n , e , and μ_i represent the ionic conductivity, concentration of charge carrier in a given volume of lattice, electronic charge, and mobility of charge carriers, respectively. In the case of pure oxygen ion conductors, ion conduction takes place via oxygen ion vacancies. Therefore, the ionic conductivity of such conductors can be also expressed as:

$$\sigma = (1 - [V_O^{\bullet\bullet}]) N_o q_i \mu_i \quad (4)$$

The N_o is the number of oxygen sites per unit volume, $V_O^{\bullet\bullet}$ represents the fraction of oxygen vacancies, and μ_i is the oxygen-ions mobility having charge denoted as q_i ^[81].

Stabilized zirconia is the most extensively investigated and most commonly used SOFC electrolyte material working at high temperatures. In order to stabilize cubic fluorite structures of zirconia, several divalent and trivalent oxide dopants are incorporated into the cation sublattice such as CaO, Y₂O₃, MgO, Sm₂O₃, Yb₂O₃. Among these compositions, 8YSZ provides the best properties for electrolyte materials, having the required characteristics for SOFC application, such as improved ionic conductivity, durability, and chemical and thermal stability in reducing and oxidizing environments^[106-108].

In further investigation of alternative electrolyte materials, Scandium-doped ceria (ScSZ) exhibits extensively higher ionic conductivity as compared to YSZ. Further, 1 mol% substitution of Bi₂O₃ in ScSZ exhibits an improved ionic conductivity of 0.33 S/cm at a temperature of 1,000 °C. At room temperature, the undoped system has a rhombohedral crystal structure, which results in lower ion conductivity compared to cubic phase structures. A cubic phase transformation occurs at higher temperatures. The 2 mol% addition of Bi₂O₃ in 10ScSZ leads to lower temperature range stability of cubic phases and exhibits the highest conductivity value (0.18 S/cm) at a temperature of 600 °C^[109]. However, the high cost of the scandium limits its practical use in SOFC applications as an electrolyte on a larger scale^[110].

Lanthanum gallate LaGaO₃-based oxides with cubic perovskite structures have been widely investigated as oxygen conductor electrolytes for IT-SOFC applications. In the crystal lattice, La³⁺ cations are situated in twelve coordination sites of O²⁻ anions, and Ga³⁺ cations occupy six-coordinated octahedral sites with the corner-sharing arrangement of GaO₆ octahedra. The GaO₆ octahedral tilting causes a deviation from ideal cubic unit cells^[111]. In order to obtain higher ionic conductivity, La can be partly substituted by Ca, Sr, Ba, Nd, and Sm, whereas Ga may also be partly substituted by Mg, Al, In, or Zn, thereby increasing the concentration of oxygen vacancies, as in LSGM. In this regard, Sr and Mg-substituted lanthanum gallate with the general formula LSGM showed a higher value of ionic conductivity than that of YSZ in the temperature range of 770-1,100 K. The TEC is also similar to the other common components of cells. The composition La_{0.8}Sr_{0.2}Ga_{0.83}Mg_{0.17}O_{3- δ} was found to exhibit a higher value of ionic conductivity ($\sigma_{\text{ion}} = 0.17 \text{ S.cm}^{-1}$ at 800 °C)^[112].

Among various oxide ion conducting electrolyte materials, the series of oxides derived from Bi₂O₃ is particularly attention-grabbing because of their high oxide ion conductivity as compared to many solid oxide electrolytes. Bi₂O₃ exhibits a noteworthy polymorphism, having α and δ as two stable phases^[113]. The δ -phase having fluorite crystal structures shows high ionic conductivity in high-temperature regions. The phase stability of the δ -phase appears above 730 °C^[111].

At temperatures below 973-1,073 K, the phase stability of the δ -Bi₂O₃ phase can be attained by doping rare-earth cations, such as Y, Er, or Dy, in bismuth and their groupings with upper oxidation state cations, for example, V, Nb, or W^[85]. The maximum ionic conductivity has been obtained in Y (Bi_{1-x}Y_xO_{1.5}, x = 0.23-0.25) and Er (Bi_{1-x}Er_xO_{1.5}, x = 0.20)-doped compounds. The Phase stability of these systems appears only in the temperature region 1,043-1,143 °C. Bi₂O₃-based materials show a number of shortcomings, such as volatilization of Bi₂O₃ at moderate temperatures, thermal instability in reducing atmospheres, high corrosion activity, and minimal mechanical strength, which affect the ion conductivity. The 20 mol% addition of Er₂O₃ in Bismuth oxide (ESB) also exhibits the maximum conductivity among all reported electrolytes of stabilized Bi₂O₃. However, ESB cannot be employed as oxide ion conductor solid electrolytes for IT-SOFCs because of its low phase stability in reducing environment $p(\text{O}_2) < 10^{-6}$ - 10^{-7} Pa at 973 K and $p(\text{O}^2) > 10^{-8}$ - 10^{-9} Pa at 873 K^[114-116].

The partial substitution of acceptor cations into the ceria lattice introduces oxygen vacancy defects that influence the ionic conductivity at relatively low operating temperatures. These defects, mainly oxygen vacancies, are responsible for influencing electrical and many other properties of solid oxides^[117,118]. In order to generate oxygen vacancies, generally, trivalent rare earth and divalent alkaline earth metals are incorporated as dopants into the ceria lattice. Among several rare earth dopants, GDC and SDC were observed as the best ionic conductors for IT-SOFCs. The value of ionic conductivity of Ce_{0.90}Gd_{0.10}O_{1.95} (CGO10) was found to be 0.01 S/cm at 500 °C^[119,120]. In the past few decades, both theoretically and experimentally, various co-doped ceria-based materials have been extensively observed as solid electrolytes for SOFC applications, such as Ce_{1-x}Ho_{0.1}Sr_xO_{2- δ} ^[121], Gd_{0.2-x}Dy_xCe_{0.8}O_{1.9}^[122], Ce_{1-a}Gd_{a-y}Sm_yO_{2-0.5}^[123], Sm_xNd_{0.15-x}Ce_{0.85}O_{2- δ} ^[124], Ce_{1-x}(Y_{0.5}Dy_{0.5})_xO_{2- δ} ^[125], Ce_{0.8}Sm_{0.2-x}Pr_xO_{2- δ} ^[126], Ce_{1-x}(Gd_{0.5}Pr_{0.5})_xO_{2- δ} ^[127], etc. Nonetheless, expensive elements in precursors, such as Sm and Gd, continue to inhibit the development of these materials as the foremost electrolytes in the SOFC market. It has been reported that the incorporation of numerous transition metal ions (Cu, Fe, Mn, Ni, Cr, Co) in minor amounts (< 1-2 mol %) into ceria serves as a sintering aid, reducing the sintering temperature and alleviating the blocking effect along GB^[128-130].

Surface and interfacial ion transport

Emerging research & development growth in the LT-SOFC field has been resulted by recent activities on the composite electrolytes, especially the doped ceria-alkali carbonate composites. One of the most important benefits of the doped ceria-carbonate composites is to resolve the problem of ceria reduction, as reported in much earlier research^[131-133]. In addition, the core-shell structure of composite electrolytes addresses the localized electrons within the ceria lattice, which are unable to travel from one particle of ceria to the other since the amorphous carbonate shell does not permit electrons to move or conduct^[90]. The description of the mechanism of charge conduction in ceria-carbonate composite materials is still not well understood. Numerous hypotheses have been proposed in recent years, and this section will provide a concise review of them. Zhu *et al.* proposed the oxide ion conduction in the oxide phase in addition to proton conduction in the carbonate salt phase in their first work on carbonate-ceria materials^[134].

Zhu *et al.* highlighted an in-depth study of oxygen ion and proton conduction mechanisms, along with the strong enhancement in conductivity^[135,136]. The most common description for the appealed interfacial superionic conductivity persists in the Maier's "space charge" layer theory^[137]. The space charge interfacial region formed along the phase boundaries as a result of the interfacial interaction between carbonate-oxide phases is usually believed to be responsible for the superior electrochemical properties; for instance, cations of the carbonate in addition to oxygen ions could accumulate along the interface. The enrichment of the

defects/ions along the interfaces rather than that of the bulk phase of ceramic essentially provides “superionic conduction highways” at the interfaces between the two constituents. Zhu *et al.* proposed that various types of negatively charged oxygen species (O_2^- , O^- , and O^{2-}) covering the oxide surface can also occur, and distinct considerations should be paid to the interfacial interactions among the oxygen ions and the alkali cations M^+ (Li^+ , Na^+ , or K^+) of the molten carbonate phase that creates an induced electrical field along the interfaces between the two phases, as shown in Figure 7^[134]. They considered that the formation of this electric field distribution plays a vital role in recognizing interfacial ionic conduction, particularly oxide ion charge conduction, permitting ions to transport along the interfaces as high conductivity highways^[134,136]. Also, Schober, using the space charge layer theory, considered that the space charge layer nearby to the interfacial region containing a higher concentration of defects than that of the bulk phases of ceramic is the main source of the superior ionic conductivity^[138]. Huang *et al.* suggested a more systematic explanation of enhanced conduction mechanisms using defect chemistry^[139]. For the alkali carbonate phase (M_2CO_3 , $M=Li, Na, \text{ or } K$), there could be a surface reaction, owing to the interfacial surface interaction, resulting in enrichment in vacancies of cation in the bulk phase of carbonate. Thus, a space charge layer is created, increasing cation disorder that offers rise to improved conductivity in ceria-carbonate composites below the melting point temperatures of the carbonate phase in the air atmosphere^[139].

SEMICONDUCTOR AND SINGLE-LAYER FUEL CELL

Literature has shown that ion conducting electrolytes with partial electronic conductivity will cause considerable losses in the cell voltage and overall system energy efficiency^[9,33,36,44]. Lots of studies have been published in the literature to overcome losses in cell voltage and system energy efficiency^[67,71,83]. Reducing electrolyte thickness from the millimeter level to the micrometer or even to the nanometer level and improving the ion conductivity of electrolytes using various thin-film technologies can result in lowered polarization loss and system efficiency for LT-SOFCs. However, due to interdiffusion between the anode and cathode materials under real-cell operational conditions, there is a growing tendency and possibility to remove the electrolyte layer, which also tackles the commercialization challenges of this thin film three-layer technology due to its complex structure and high cost^[89,140].

Recently discovered SLFC or EFFC devices have attracted lots of attention to overcome the limitations of three-layer structures, which showed lower ionic conductivity at a low-temperature regime (300–600 °C)^[17,18,38,51,141–144]. Figure 8 illustrates the conventional three-layer configuration of a SOFC with oxygen ion conducting electrolytes without electron passage, SLFC configuration, and configurations for the dual-component SLFC device.

As can be seen in Figure 8A, the H_2 fuel is oxidized, and electrons are released at the anode side. Further, oxygen is reduced to oxygen ions (O^{2-}) at the cathode side, which combine with electrons from the external circuit to produce electricity. Interestingly, the SLFC device [Figure 8B] can show even better performance than the electrolyte-based SOFC device. As a result, SLFC demonstrates great potential for further advancement and needs in-depth investigation to prove its utility. The working principle of the SLFC is described below^[17].

SLFC features a homomorphous layer structure comprising a combination of semiconductors and oxygen ion conductors or heterostructure composite materials. This unique composition enables the SLFC to exhibit the same fuel cell functionality or better performance as compared to traditional designs, encompassing ion transport and facilitating the necessary ion/electron junction and function between the anode/electrolyte and electrolyte/cathode. SLFC can perform operations in a temperature range of 300 to 600 °C. Remarkably, this single layer can deliver the same or better performance in comparison to complex three-layer fuel cells.

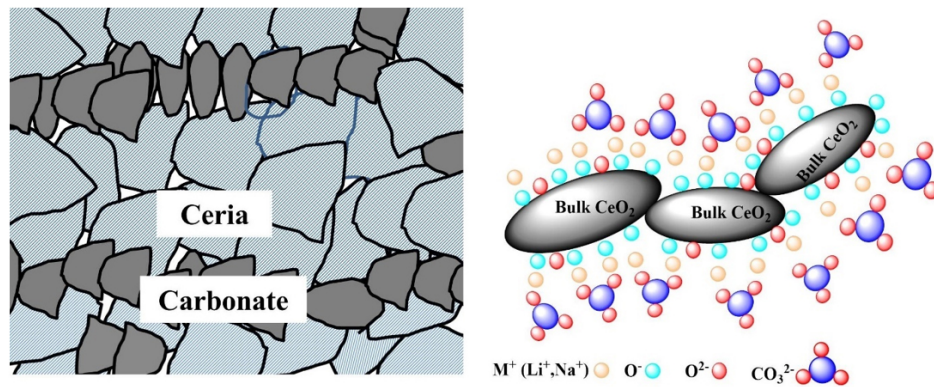


Figure 7. Interfacial superionic charge conduction pathway based on space charge layer theory. Adopted and modified from Ref. ^[134].

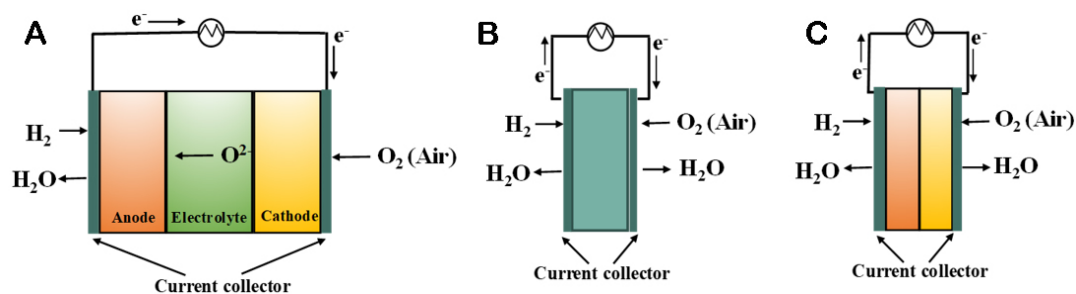


Figure 8. Schematics of a (A) conventional Solid oxide fuel cell (SOFC) configuration, (B) single-component fuel cell (SLFC) device configurations, and (C) dual-component SLFC device configuration. Redrawn with permission from Ref. ^[17].

It is widely acknowledged in the scientific community that in a conventional SOFC, electronic conduction through the electrolyte/membrane can significantly reduce both the cell voltage (OCV) and overall system energy efficiency. Also, in SLFC, electronic conduction has no impact on the behavior of the fuel cell. This simply implies that the energy conversion mechanism differs in semiconductor-based fuel cells and ion electrolyte membrane-based fuel cells. The advent of SLFC introduces a new direction for SOFC research by enabling the development of electrolyte-free devices. In detail, the working principle of the SLFC has been elucidated in the work by Zhu *et al.* ^[17,89,142,143].

SLFC technology has many similarities with the characteristics of a dye solar cell, which also uses a mixture of electronic and ionic conductors (electrolytes). SLFC consists of two basic phases of ionic materials and semiconducting materials in a single layer. Both phases form a composite with percolation paths for ions and electrons. The ionic conductive behavior may resemble a normal electrolyte process, while for electrons, there may be a *p-n* junction in the single-layer device. In fact, the functional composite layer consists of *n*- and *p*-type semiconductors. When H_2 and air are supplied to the SLFC, a series of electrochemical processes occur. The H_2 molecules are adsorbed onto the surface of the *n*-type semiconductor particles, where they undergo dissociation, resulting in the generation of H^+ ions. Simultaneously, the O_2 molecules from the air are adsorbed onto the surface of the *p*-type semiconductor particles and dissociated into O^{2-} ions. Due to the surface reactions, negative charges (electrons) accumulate at the surface of the *n*-type semiconductors, while positive charges (holes) accumulate at the surface of the *p*-type semiconductors. However, the junction region between the *n*-type and *p*-type semiconductors is depleted of charge carriers, creating a non-conductive barrier for electrons. This charge separation and depletion region at the *p-n* junction creates a

potential difference, leading to the generation of a cell potential. This potential difference allows the flow of electrical current when an external circuit is connected, enabling the extraction of electrical energy from the SLFC device. This principle is comparable to a solar cell and, thus, avoids the problems of short circuits and self-discharge^[18]. This will be further discussed in the following section.

As explained above, an EFFC is an innovative energy conversion device that offers numerous advantages compared to traditional SOFCs due to their distinct operating mechanisms^[17,51,141,142]. Here are some key advantages of EFFCs:

(i) Significant reduction in fabrication costs: EFFCs feature a simple structure and preparation method, leading to lower fabrication costs compared to conventional SOFCs.

(ii) Elimination of interface losses: EFFCs eliminate the polarization losses associated with the two interfaces, namely the electrolyte/anode and electrolyte/cathode, present in the trilayer structure of traditional SOFCs. The absence of these interfaces in EFFCs allows for improved long-term stability and avoids losses or thermal stresses at the interfaces.

(iii) Enhanced redox reactions: EFFCs enable efficient redox reactions, such as the hydrogen oxidation reaction (HOR) and oxygen reduction reaction (ORR), to occur directly within the single layer. This facilitates more efficient ion transport, enhancing the performance of the fuel cell reactions.

(iv) Built-in field for improved efficiency: EFFCs generate a built-in field at the anode (n) and cathode (p) junction, promoting the transfer of O^{2-} and H^+ ions. This improved ion transfer contributes to enhancing the overall efficiency of the cell.

In summary, EFFCs offer advantages such as reduced fabrication costs, elimination of interface losses, enhanced redox reactions, and the presence of a built-in field, all of which contribute to improved efficiency and long-term stability compared to traditional SOFCs. The unique characteristics of semiconductors and heterostructures enable precise control and manipulation of charge carrier dynamics and electrochemical processes. These materials facilitate efficient ion transport and enable redox reactions at the nanoscale, leading to improved fuel cell performance and increased understanding of fundamental electrochemical processes.

Recent progress in EFFCs revealed that the electrochemical performance is influenced by various factors, including the characteristics of the starting materials, stoichiometric ratios, compositions between ionic conductors and semiconductors, morphology, microstructures, and sintering or experimental conditions. EFFC materials predominantly consist of composites composed of two different types of constituents. One of these constituents is oxide ionic conductors, such as Sm_2O_3 -doped CeO_2 (SDC)^[98], Gd_2O_3 -doped CeO_2 (GDC)^[143], and other ceria-based composites. These oxide ionic conductors play a crucial role in facilitating ion transport within the EFFC system. For instance, Hu *et al.* employed MgZn-SDC materials as a single-component oxide layer in EFFCs^[97]. This MgZn-SDC material demonstrated favorable electrochemical properties and offered potential cost reduction benefits due to simple fabrication. Also, by introducing Mg and Zn contents, the cost of this type of material could be further lowered, enhancing its economic viability for EFFC applications.

Semiconducting materials, including various transition metal oxides such as NiO, CuO, FeO_x, ZnO, CoO_x-doped LiNiO₂, *etc.*, have shown potential in EFFC research. In particular, Zhu *et al.* demonstrated the combination of semiconductor materials, such as LiNiO₂, with ionic conductor such as GDC to fabricate an EFFC device^[143]. This hybrid approach resulted in an EFFC device achieving a maximum power density of 450 mW/cm² at an operating temperature of 550 °C^[143]. Further, researchers have explored various composite materials for EFFC devices. One notable material is LiNiZnO_{2-δ}-SDC, which demonstrated an impressive maximum power output of up to 600 mW/cm² at 550 °C^[18]. Additionally, ceria-carbonate materials were utilized by Zhu *et al.* to produce semiconductor ion single-layer materials, resulting in a remarkable maximum power output of 700 mW/cm² at 550 °C when mixing LiNiCuZnFe oxide and Na₂CO₃-SDC (NSDC) composites^[144]. Another significant development by Dong *et al.* involved the creation of a single-layer material for EFFC using a specific mass ratio of Sr₂Fe_{1.5}Mo_{0.5}O_{6-δ} (SFM) and NSDC^[145].

Later, developments have widely explored semiconductor ion materials (SIMs) and devices. The concept of SIMs defines new functional materials to demonstrate the SIFC. It is known that mixed ionic and electronic conductors (MIECs) exist, and there is a theory that if the MIEC was used as a fuel cell membrane to replace the electrolyte, it could cause the device OCV to decrease below the Nernst value and performance significant losses. Several semiconductor materials have been used as fuel cell membranes of SLFCs in the same way, e.g., Li_xAl_{0.5}Co_{0.5}O₂^[54,146], SmNiO₃^[147], TiO₂^[100], BaSnO₃^[148], and NBT^[12]. In many SIMs, two material structures are very interesting, such as the materials with perovskite structures, LSCT^[149], LaSrCoFeO₃^[31] and LaSrCrFeO_{3-d}^[150], which form a composite with doped ceria, and NdBa_{0.5}Sr_{0.5}Co_{1.5}Fe_{0.5}O_{5+d}^[151], which forms a composite with BZCY as an electrolyte for SLFCs. It has been generally confirmed that electron conduction through the electrolyte/membrane causes significant losses in both cell voltage (OCV) and energy efficiency of the classical SOFC, while it does not affect the fuel cell performance of the solid-state fuel cell. Another important characteristic is balanced electron and ion conductivity so that the fuel cell device can operate without short circuit problems and provide good performance^[31].

In developing SIFC devices, we have taken advantage of semiconductor materials and fabricated junction devices by inserting a thin semiconductor layer, e.g., LiNi_{0.8}Co_{0.15}Al_{0.05}O₂ (NCAL), with metal current collectors Ni or Ag in the Ni/NCAL/semiconductor ion composite/NCAL/Ni configuration. These devices are designed using energy band, band alignment, and junction technologies. Using the energy band design and approach, the devices have been largely developed using semiconductor band materials and their heterostructure composites to replace the conventional ionic electrolyte, combined with NCAL as electron/hole transport materials and redox reaction electrodes^[28].

BAND STRUCTURE, BAND ALIGNMENTS, AND BUILT-IN-FIELD EFFECTS IN SEMICONDUCTOR ELECTROLYTES

In these semiconductor-based heterostructure membrane devices, a key challenge is how to block the electronic conduction transition to an internal device. Therefore, several semiconductor junction devices have been developed, which contribute interesting and important content to semiconductor electrochemistry.

Schottky junction

In subsequent advancements of fuel cell technology, the SJ became a pivotal component with a profound impact on fuel cell performance, as SJ-based fuel cells are a cost-effective and straightforward fuel cell technology. Notably, the SJ fuel cell device, as depicted in [Figure 9](#), employs a single semiconductor, commonly *n*-type or *p*-type, or heterostructure^[28]. A potential difference can be easily established at the interface between a metal and an *n*- or *p*-type semiconductor, commonly known as a Schottky barrier, in an

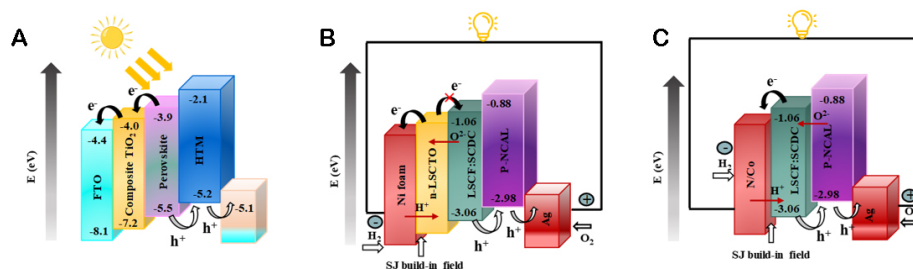


Figure 9. Energy level diagram of (A) perovskite solar cells, (B) the fuel-to-electricity conversion device inspired by Perovskite solar cell structures (Type I), and (C) symmetrical fuel-to-electricity conversion device (Type II) with an *in-situ* formed Schottky junction. Adapted and modified from Ref. [28].

SJ fuel cell device. Various types of SJ devices, including solar cells and sensors, have been developed using this concept and taking advantage of the depletion layer that forms between the metal and the semiconductor. A well-known function of SJ is to separate electron/hole pairs by establishing an internal device voltage. The formation of a Schottky barrier occurs between the surface of the anodically reduced metal and the semiconductor in a fuel cell.

Figure 10 shows the operating mechanism of the $\text{Ce}_{0.8}\text{Sm}_{0.2}\text{O}_{2-\delta}$ and SrTiO_3 (SDC-STO) fuel cell based on the SJ effect and defines the energy band that builds up across the junction [82]. The SJ is formed *in-situ* by the reduced metallic Ni/Co from NCAL on the H_2 side at the NiCo/STO and NiCo/SDC interfaces. The barrier of SJ plays a vital role in electronic suppression to avoid the short circuit issue [82]. This is similar to the junction described for the NCAL and LZO-SDC systems [152].

***p-n* heterojunction**

As previously mentioned, the elimination of the intermediate electrolyte layer from a conventional SOFC allows the fuel cell to transform into a *p-n* junction-based device. In the study conducted by He *et al.* in 2000 [91], SLFC was fabricated using $\text{La}_{0.9}\text{Sr}_{0.1}\text{InO}_{3-\delta}$ as the functional single layer, exhibiting *p* and *n*-type conduction at high and low oxygen partial pressures. This SLFC behavior closely resembles the traditional SOFC, wherein the *p*- and *n*-type conduction properties are crucial for electrode functionality.

This SLFC-based fuel cell is also highlighted by Singh *et al.* [20]. Generally, a fuel cell device can be considered as an assembly consisting of *n* (anode), *p* (cathode), and an ionic conducting electrolyte/component, as shown in Figure 11A, with material aspects. If the middle electrolyte layer is removed, Figure 11A transforms into a *p-n* junction-based fuel cell device [Figure 11B]. Asghar *et al.* have also confirmed that wide bandgap semiconductors can be used as an ionic electrolyte material [22]. It means that a SOFC could be conceptually treated as a semiconductor fuel cell system, while the fuel cell effectively functions as a *p-n* junction device by removing the middle electrolyte layer of the SOFC [Figure 11B]. As expected, SLFC showed the same functions or performances as the traditional SOFC but can be designed with different configurations.

Band alignments

The electrochemical reaction and charge transfer processes in a fuel cell device involve two half-cell reactions (oxidation and reduction) from both sides of the electrolyte interfaces. The anode and cathode sides of the electrochemical cell separate electron-hole pairs (e^-/h^+) through the band structure, encompassing the conduction band (CB), valence band, and BIEF. This energy band serves as a crucial pathway for the electrochemical reaction. Within the anode and cathode's CB (EC) and valence band (EV), free electrons and holes engage in charge exchange with the electrolyte via diffusion-based processes,

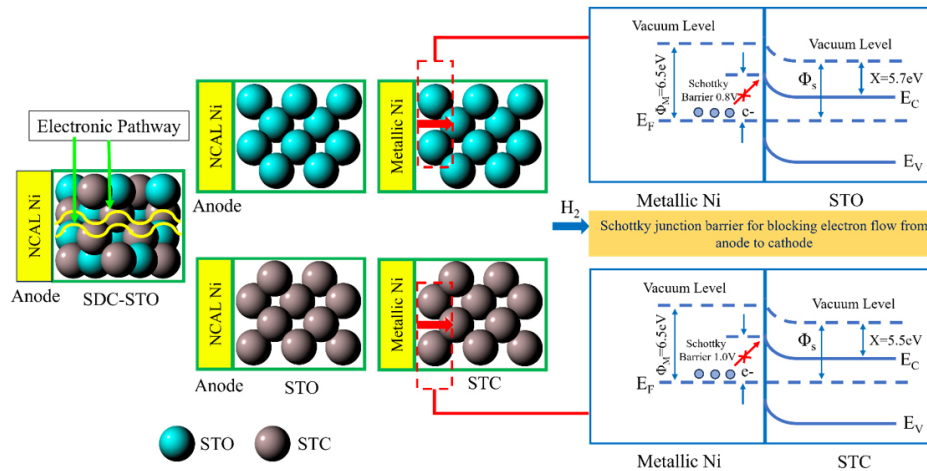


Figure 10. Schematic diagram of the $\text{Ce}_{0.8}\text{Sm}_{0.2}\text{O}_{2.8}$ and SrTiO_3 (SDC-STO) fuel cell that reveals the electronic blocking mechanism by Schottky junction effect at anodic NiCo/electrolyte interface. Adapted and modified from Ref. [82].

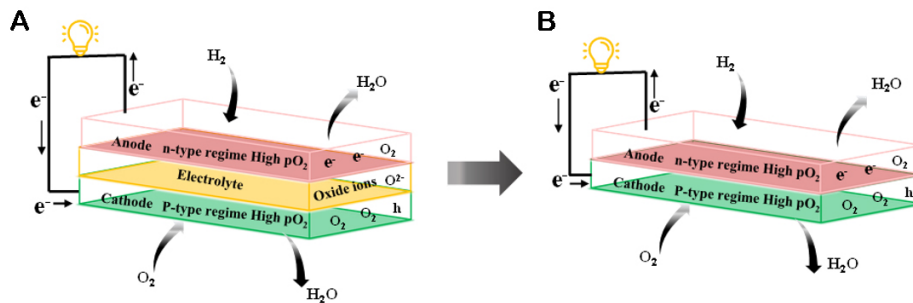


Figure 11. Transition of fuel cell from (A) ionic conductor-based materials to (B) p - n junction assembly. Adapted and modified from Ref. [89].

facilitating charge neutrality at the interface. Consequently, these processes induce a reconfiguration of the energy band structures, resulting in band bending, a phenomenon known as energy band alignment, which manifests within fuel cells. In semiconductors, the position of the Fermi level (E_F) predominantly relies on the type of doping (n -type or p -type). Additionally, there are no alternative reference energy states to access energy levels; thus, the position of E_F can only be determined if the distances between E_F , E_C , or E_V are known.

Generally, two types of band bending can occur, namely upward band bending and downward band bending, which depend on the material's nature and the modification of the energy band structure near the surface or interface of a material. Regarding an n -type semiconductor (anode), the E_F typically resides at a higher energy compared to that of the electrolyte. Consequently, electrons tend to migrate from the semiconductor (anode) toward the electrolyte in order to equalize the E_F s. This process causes the E_F of semiconductors to gradually decrease in energy until both levels align, resulting in a shift of E_F to a lower energy (down-band bending). The corresponding illustration in Figure 12 visually depicts this phenomenon, showcasing the creation of a potential barrier for electrons. As a result, their movement is impeded, leading to the formation of a depletion layer near the surface of the semiconductor. Conversely, for p -type semiconductors, the E_F is usually positioned at a lower energy (near the valence band) relative to the electrolyte. As a result, the E_F shifts to higher energy (up-band bending) at the interface. To establish

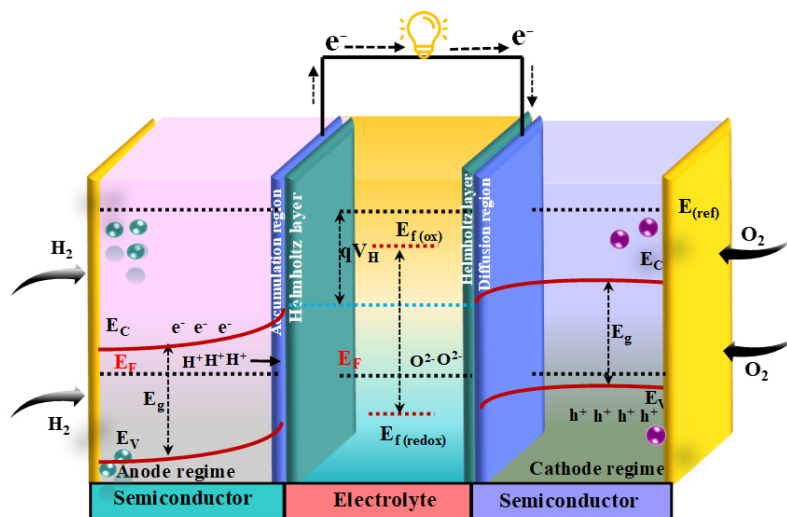


Figure 12. Schematic of the working principle and energy diagram for a solid oxide fuel cell electrode (semiconductors) interface with electrolytes in Fermi level equilibrium. Adapted and modified from Ref. [89].

electronic equilibrium, an electron deficiency (h^+) occurs near the anode surface within the positive space charge region as electrons are transferred to the electrolyte. This positive space charge signifies a scarcity of electrons within this specific region.

Accordingly, the energy gap between the E_F and the CB is increased at the interface, resulting in a corresponding band bending; therefore, a charge accumulation depletion region is formed on the semiconductor side (anode). Conversely, when the electrolyte side reaches full charge, unabsorbed ions of opposite charges persist at the electrolyte interface, giving rise to the formation of a Helmholtz bilayer, as depicted in Figure 12. Due to the disparity in electrostatic potential during the process, a space charge zone is anticipated on the semiconductor side, resulting in a shift in the position of the E_F . As a consequence, charge transfer occurs from the space charge zone toward the electrolyte, leading to energy loss and subsequent reorganization of the band structure (refer to Figure 12).

The space charge zone (created by the change of E_F positions) can be anticipated on the semiconductor side because of the difference in electrostatic potential created during the process, causing the transfer of charges to the electrolyte; as a result, the semiconductor loses its energy, leading to a rearrangement in the band structure (see Figure 12). The potential difference between the semiconductor and the electrolyte has an influence on the concentration of charges in the space charge region. The potential drop within the space charge region is notably greater than that of the Helmholtz layer. This discrepancy arises due to the extensive ionization of the acceptor solid, which covers a wide area, in contrast to the ions situated far from the electrolyte surface that form the Helmholtz layer. The non-uniform distribution of charges in the interfacial region results in the formation of a BIEF that extends across the electrode/electrolyte interface. This BIEF can facilitate the movement of ions or charge carriers across the interface, albeit necessitating some energy. In simpler terms, the produced electric field possesses an inherent potential difference. The significance of this inherent potential at the interface is its role in impeding the movement of electrons and holes across the junction, establishing a potential barrier that determines the voltage of the device. In real-world applications, it may be a single interface, and the built-in field exists because of the advanced technology used to construct the device with an electrode in more or less ohmic contact to reduce polarization loss.

The utilization of band alignments and junctions in fuel cells, which are constructed using energy bands of semiconductors and heterostructure materials, plays a crucial role in optimizing the efficiency of fuel conversion^[153]. Although ion and electron conduction coexist in the heterostructure semiconductor membranes, there is no electronic short-circuit issue due to the design energy band, and the alignment forming the junction plays a key role in preventing the electrons from passing through the internal devices while generating high power outputs $> 1,000 \text{ mW cm}^{-2}$ at $550 \text{ }^\circ\text{C}$. By lowering the necessary activation energy, band alignment can significantly enhance the efficiency of the electrode HOR and ORR processes. This phenomenon is frequently observed in the realm of photoelectrochemical water splitting. This approach holds promise as a universal method for advancing the performance of semiconductor-based conversion devices.

Built-in-field effects

A unique feature of the compound properties is the formation of a built-in field that can promote the transport of ions (H^+ or O^{2-}). Assuming no voltage is applied to the p - n junction, the junction attains thermal equilibrium, where the Fermi energy level remains constant throughout the system. **Figure 13** illustrates the energy band diagram for the p - n junction under thermal equilibrium. As the conduction and valence band energies traverse the space charge region, they undergo bending due to the changing relative position between the conduction and valence bands with respect to the Fermi energy in the p - and n -domains. Electrons in the n -region CB encounter a potential barrier while entering the p -region CB. This potential barrier is called the built-in potential barrier. This barrier preserves the equilibrium between the majority carrier electrons in the n -region and the minority carrier electrons in the p -region and between the majority carrier holes in the p -region and the minority carrier holes in the n -region. Since the potential preserves equilibrium, no current is generated at this voltage. Due to the transition, the intrinsic EF is equally distant from the CB edge. Therefore, the difference between the intrinsic EFs in the p and n regions can be used to determine the built-in potential barrier^[154].

SUMMARY AND REMARKS/PERSPECTIVE

Solid oxide fuel cell (SOFC) route towards semiconductor membrane fuel cell (SMFC) from material aspects

Since the last few decades, the three layers, anodes, electrolytes, and cathodes, of conventional SOFCs have been continuously modified with new materials, especially electrolyte and cathode materials. In SOFC technology, basic requirements for suitable electrolyte materials, which are sandwiched between anodes and cathodes, include several factors: sufficient high oxygen ionic conductivity (0.1 S/cm) at operating temperatures, compatibility with electrodes, prevention of electronic conduction, adequate mechanical properties, and thermodynamic and chemical stability.

Various materials developed for electrolytes are fluorite-structure-type-based, such as ZrO_2 , CeO_2 , and Bi_2O_3 , and perovskite-structure-based, which mainly includes LaGaO_3 , and pyrochlore^[50,155]. Despite the fact that all these fluorite-type and perovskite-structure-based electrolytes are being used as SOFC electrolytes, YSZ electrolyte-based SOFC is the only available commercial product in the market. The operating temperature of YSZ-based SOFC should be 700 - $1,000 \text{ }^\circ\text{C}$ to get sufficiently high fuel cell performance (if no thin film technology is involved). High temperature operation and complex technology results in high-cost manufacturing.

Interestingly, all these advanced SOFC materials developed can be applied in SMFCs using both electrode and electrolyte membranes. Here, both electrode and electrolyte membranes are based on semiconductors for SMFCs and have shown no compatibility issue. These types of SMFCs can easily avoid compatibility issues between the electrolyte and electrode as an electrolyte itself contains the electrode with good

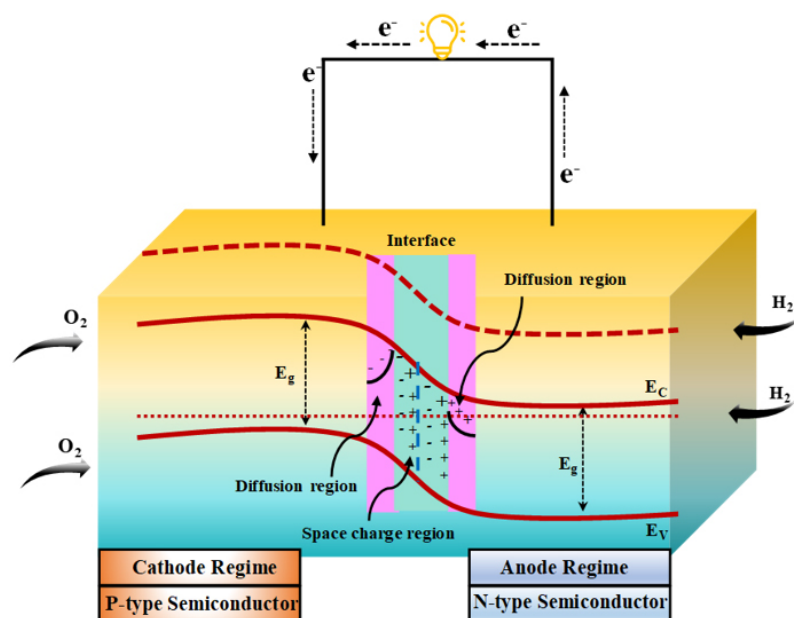


Figure 13. Energy-band diagram of a p - n junction formed in thermal equilibrium. Adapted and modified from Ref. [89].

compatibility. Also, developed compatible SMFC electrode materials showed better catalytic activity and redox ability, which helps improve the performance and durability of SMFC devices.

Further, conventional SOFCs are high temperature manufacturing technology, and their electrolytes have limited flexibility towards electrode materials. Contrary, SMFC technology is considered low-cost manufacturing and a wide range of materials, which are based on semiconductors/metal oxide semiconductors, such as ZnO, TiO₂, NiO, CuO, and perovskite-type oxide, such as SrTiO₃, SrCoSnO₃, etc. In particular, SOFC perovskite cathode materials, which are usually p -type semiconductors, can function as electrolytes following the SJ principle. Semiconductor-based electrolytes exhibit some electronic conduction, which makes SMFCs work with better performance based on the junction principle due to high ionic conductivity of 0.1 S/cm in a low-temperature range (< 500 °C) [18,52,87]. More research and development efforts are needed to work on the current limitations and issues related to SMFC-based devices, e.g., long-term stability, scalability, etc. By designing novel materials, new fabrication technologies, advanced synthesis routes, and new technologies, these limitations can be addressed, and we may realize better functioning and enhanced overall efficiency of SMFC devices.

Solid oxide fuel cell (SOFC) towards SMFC from technologies aspects

Thin film fabrication of SOFCs using physical and chemical methods, such as pulsed laser deposition, ALD, chemical vapor deposition, physical vapor deposition, atmospheric plasma spraying, and sol-gel, results in better fuel cell performance in the low-temperature range of 600 °C when compared to bulk electrolyte-supported SOFCs [156,157]. The internal resistance of the device is decreased due to these thin-film technologies. In contrast to bulk electrolyte-supported SOFCs, thin film-fabricated SOFCs have durability issues for long-life operation. The expensive and challenging nature of the thin film fabrication process is another drawback. For long-life SOFC products (over 40,000 h), reliable thick-electrolyte-supported technologies serve as the foundation. Contrary to thin film fabrication techniques, the low-cost bulk shaping technique is well suited for use in advanced SMFCs and has a number of benefits, including minimal power loss due to interfacial polarization and simple cell fabrication. For example, perovskite materials, which are

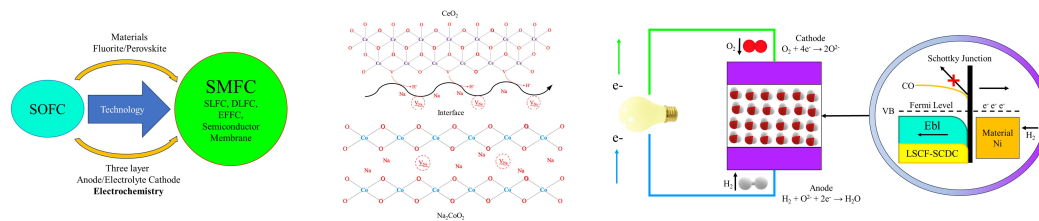


Figure 14. Schematic representation of Solid oxide fuel cell (SOFC) shifting towards Semiconductor membrane fuel cell (SMFC) from materials, technologies, and science aspects.

used as cathode components in conventional SOFCs, can be used as the semiconductor electrolyte membrane in SMFC without having any interfacial gap problems. This interfacial issue is predominant in SOFC technology and results in lots of disadvantages, e.g., major power loss.

Here, in the fabrication of SMFCs, the semiconductor electrolyte membrane, LSCF-Sm/Ca co-doped CeO_2 (SCDC) nanocomposites, is sandwiched between the two NCAL thin electrode layers; i.e., Symmetrical electrodes are applied to the SMFC device, as shown in Figure 14^[158,159]. Also, in SMFC, the cell is easy to fabricate, compared to SOFC, by shaping drying powder into pellets under applied pressure without using the high-temperature sintering densification method as in SOFC. Here, the intrinsic semiconductor and heterostructure material layer is used as a key layer in SMFCs rather than the ionic-conductive electrolyte layer as in SOFCs. The key issue difference for SMFCs is the low temperature ($= 600\text{ }^\circ\text{C}$)-treated semiconductor-based functional layer, whereas the SOFC requires a high temperature ($\geq 1,300\text{ }^\circ\text{C}$) treatment with a multi-step co-sintering process. Moreover, the SMFC can also be designed by a material of single layers of conventional SOFC cathode components to realize SOFC anode, electrolyte, and cathode three-component functions, which leads to simple fuel cell advanced technology. Additionally, the advanced engineering of the SMFC device will be crucial not only for its scalability but also for unlocking its full potential.

SOFCs towards SMFCs from cost and commercialization aspects

From a commercial point of view, the cost of SOFCs mainly depends on fuel cell stack cost, which depends on factors such as material cost, machining cost, energy cost, bipolar plates, and labor cost^[160,161]. Among these different expenses, the materials cost of SOFCs and bipolar plates constitutes the majority portion of the total cost for the fuel cell stack. Also, conventional SOFCs operate at temperatures above $700\text{ }^\circ\text{C}$, so the cost of bipolar plates is much higher than that of SMFCs due to the use of special and expensive alloy materials.

Future research and development may be focused on Semiconductor-ionic-based materials to develop next-generation functional materials by combining semiconductor energy band and BIEF theories to design and develop new-generation superionic materials with self-field driven ionic transport at low temperatures ($300\text{--}500\text{ }^\circ\text{C}$). Further, advanced research should focus on fuel cell devices based on semiconductor band alignment and the BIEF effect, which can improve HOR and ORR and charge (electrons and ions) transfer and ion transport. These advancements are aimed at enhancing fuel cell performance, lowering device costs, and creating a vital alternative path for commercialization.

DECLARATIONS

Acknowledgments

The authors gratefully acknowledge Dr. Ashish Kumar Singh from Guru Ghasidas Vishwavidyalaya, Bilaspur, Chhattisgarh, and Rohan Gupta, a final-year undergraduate student from the Indian Institute of Technology Patna, India, for their assistance with figure redrawing.

Authors' contributions

Collaborating on the writing and revision of the paper with the help of all the authors: Singh M (Manish Singh), Paydar S

Conceived the structural idea and supervised the manuscript, performed drafting and editing of the manuscript: Singh M (Manish Singh), Singh M (Monika Singh)

Redrew, arranged all the figures, and helped with editing: Singh A, Singhal R

All authors discussed the results and contributed to the manuscript.

Availability of data and materials

Not applicable.

Financial support and sponsorship

None.

Conflict of Interest

All authors declared that there are no conflicts of interest.

Ethical approval and consent to participate

Not Applicable

Consent for publication

Not applicable.

Copyright

© The Author(s) 2024.

REFERENCES

1. Höök M, Tang X. Depletion of fossil fuels and anthropogenic climate change - a review. *Energy Policy* 2013;52:797-809. DOI
2. Abdalla AM, Hossain S, Azad AT, et al. Nanomaterials for solid oxide fuel cells: a review. *Renew Sustain Energy Rev* 2018;82:353-68. DOI
3. Suntivich J, Gasteiger HA, Yabuuchi N, Nakanishi H, Goodenough JB, Shao-horn Y. Design principles for oxygen-reduction activity on perovskite oxide catalysts for fuel cells and metal-air batteries. *Nat Chem* 2011;3:546-50. DOI
4. Singhal SC. Solid oxide fuel cells for power generation. *WIREs Energy Environ* 2014;3:179-94. DOI
5. Jiang S, Zhou W, Niu Y, Zhu Z, Shao Z. Phase transition of a cobalt-free perovskite as a high-performance cathode for intermediate-temperature solid oxide fuel cells. *ChemSusChem* 2012;5:2023-31. DOI PubMed
6. Holtappels P, Stimming U. Solid oxide fuel cells (SOFC). In: Vielstich W, Lamm A, Gasteiger HA, Yokokawa H, editors. Handbook of fuel cells. Hoboken: Wiley; 2010. DOI
7. Fan L. Solid-state electrolytes for SOFC. In: Zhu B, Raza R, Fan L, Sun C, editors. Solid oxide fuel cells. Hoboken: Wiley; 2020. pp. 35-78. DOI
8. Lacerda M, Irvine JTS, Glasser FP, West AR. High oxide ion conductivity in Ca₁₂Al₁₄O₃₃. *Nature* 1988;332:525-6. DOI
9. Nakayama S, Kageyama T, Aono H, Sadaoka Y. Ionic conductivity of lanthanoid silicates, Ln₁₀(SiO₄)₆O₃ (Ln = La, Nd, Sm, Gd, Dy, Y, Ho, Er and Yb). *J Mater Chem* 1995;5:1801-5. DOI
10. Lacorre P, Goutenoire F, Bohnke O, Retoux R, Laligant Y. Designing fast oxide-ion conductors based on La₂Mo₂O₉. *Nature* 2000;404:856-8. DOI PubMed
11. Haugsrud R, Norby T. Proton conduction in rare-earth ortho-niobates and ortho-tantalates. *Nat Mater* 2006;5:193-6. DOI
12. Li M, Pietrowski MJ, De Souza RA, et al. A family of oxide ion conductors based on the ferroelectric perovskite Na_{0.5}Bi_{0.5}TiO₃. *Nat Mater* 2014;13:31-5. DOI
13. Singh P, Goodenough JB. Monoclinic Sr_{1-x}Na_xSiO_{3-0.5x}: new superior oxide ion electrolytes. *J Am Chem Soc* 2013;135:10149-54. DOI PubMed
14. Fan L, Zhu B, Su P, He C. Nanomaterials and technologies for low temperature solid oxide fuel cells: recent advances, challenges and opportunities. *Nano Energy* 2018;45:148-76. DOI

15. Zhu B, Albinsson I, Andersson C, Borsand K, Nilsson M, Mellander B. Electrolysis studies based on ceria-based composites. *Electrochem Commun* 2006;8:495-8. DOI
16. Fan L, Zhang G, Chen M, Wang C, Di J, Zhu B. Proton and oxygen ionic conductivity of doped ceria- carbonate composite by modified Wagner polarization. *Int J Electrochem Sci* 2012;7:8420-35. DOI
17. Zhu B, Raza R, Qin H, Liu Q, Fan L. Fuel cells based on electrolyte and non-electrolyte separators. *Energy Environ Sci* 2011;4:2986-92. DOI
18. Zhu B, Raza R, Abbas G, Singh M. An electrolyte-free fuel cell constructed from one homogenous layer with mixed conductivity. *Adv Funct Mater* 2011;21:2465-9. DOI
19. Garcia-barriocanal J, Rivera-calzada A, Varela M, et al. Colossal ionic conductivity at interfaces of epitaxial $\text{ZrO}_2\text{:Y}_2\text{O}_3\text{/SrTiO}_3$ heterostructures. *Science* 2008;321:676-80. DOI
20. Singh K, Nowotny J, Thangadurai V. Amphoteric oxide semiconductors for energy conversion devices: a tutorial review. *Chem Soc Rev* 2013;42:1961-72. DOI PubMed
21. Götsch T, Bertel E, Menzel A, Stöger-pollach M, Penner S. Spectroscopic investigation of the electronic structure of yttria-stabilized zirconia. *Phys Rev Mater* 2018;2:035801. DOI
22. Asghar MI, Jouttijärvi S, Jokiranta R, Valtavirta A, Lund PD. Wide bandgap oxides for low-temperature single-layered nanocomposite fuel cell. *Nano Energy* 2018;53:391-7. DOI
23. Adler SB. Factors governing oxygen reduction in solid oxide fuel cell cathodes. *Chem Rev* 2004;104:4791-843. DOI PubMed
24. Sunarso J, Hashim SS, Zhu N, Zhou W. Perovskite oxides applications in high temperature oxygen separation, solid oxide fuel cell and membrane reactor: a review. *Prog Energy Combust Sci* 2017;61:57-77. DOI
25. Liu D, Kelly TL. Perovskite solar cells with a planar heterojunction structure prepared using room-temperature solution processing techniques. *Nat Photon* 2014;8:133-8. DOI
26. Oikawa T, Ohdaira K, Higashimine K, Matsumura H. Application of crystalline silicon surface oxidation to silicon heterojunction solar cells. *Curr Appl Phys* 2015;15:1168-72. DOI
27. Wu S, Li L, Wang W, et al. Study on the front contact mechanism of screen-printed multi-crystalline silicon solar cells. *Sol Energy Mater Sol Cells* 2015;141:80-6. DOI
28. Zhu B, Huang Y, Fan L, et al. Novel fuel cell with nanocomposite functional layer designed by perovskite solar cell principle. *Nano Energy* 2016;19:156-64. DOI
29. Zhu B, Lund P, Raza R, et al. A new energy conversion technology based on nano-redox and nano-device processes. *Nano Energy* 2013;2:1179-85. DOI
30. Xia C, Mi Y, Wang B, Lin B, Chen G, Zhu B. Shaping triple-conducting semiconductor $\text{BaCo}_{0.4}\text{Fe}_{0.4}\text{Zr}_{0.1}\text{Y}_{0.1}\text{O}_{3-\delta}$ into an electrolyte for low-temperature solid oxide fuel cells. *Nat Commun* 2019;10:1707. DOI PubMed PMC
31. Zhu B, Wang B, Wang Y, et al. Charge separation and transport in $\text{La}_{0.6}\text{Sr}_{0.4}\text{Co}_{0.2}\text{Fe}_{0.8}\text{O}_{3-\delta}$ and ion-doping ceria heterostructure material for new generation fuel cell. *Nano Energy* 2017;37:195-202. DOI
32. Zhang Y, Liu J, Singh M, et al. Superionic conductivity in ceria-based heterostructure composites for low-temperature solid oxide fuel cells. *Nanomicro Lett* 2020;12:178. DOI PubMed PMC
33. Takahashi T, Esaka T, Iwahara H. Conduction in Bi_2O_3 -based oxide ion conductor under low oxygen pressure. II. Determination of the partial electronic conductivity. *J Appl Electrochem* 1977;7:303-8. DOI
34. Zhu B, Mi Y, Xia C, et al. A nanoscale perspective on solid oxide and semiconductor membrane fuel cells: materials and technology. *Energy Mater* 2021;1:100002. DOI
35. Zakaria Z, Abu Hassan SH, Shaari N, Yahaya AZ, Boon Kar Y. A review on recent status and challenges of yttria stabilized zirconia modification to lowering the temperature of solid oxide fuel cells operation. *Int J Energy Res* 2020;44:631-50. DOI
36. He L, Su Y, Lanhong J, Shi S. Recent advances of cerium oxide nanoparticles in synthesis, luminescence and biomedical studies: a review. *J Rare Earths* 2015;33:791-9. DOI
37. Bhalla AS, Guo R, Roy R. The perovskite structure - a review of its role in ceramic science and technology. *Mater Res Innov* 2000;4:3-26. DOI
38. Wang Z, Meng Y, Singh M, et al. Ni/NiO exsolved perovskite $\text{La}_{0.2}\text{Sr}_{0.7}\text{Ti}_{0.9}\text{Ni}_{0.1}\text{O}_{3-\delta}$ for semiconductor-ionic fuel cells: roles of electrocatalytic activity and physical junctions. *ACS Appl Mater Interfaces* 2023;15:870-81. DOI
39. Shao K, Li F, Zhang G, Zhang Q, Maliutina K, Fan L. Approaching durable single-layer fuel cells: promotion of electroactivity and charge separation via nanoalloy redox exsolution. *ACS Appl Mater Interfaces* 2019;11:27924-33. DOI
40. Sunarso J, Baumann S, Serra J, et al. Mixed ionic-electronic conducting (MIEC) ceramic-based membranes for oxygen separation. *J Membr Sci* 2008;320:13-41. DOI
41. Ali R, Yashima M. Space group and crystal structure of the perovskite CaTiO_3 from 296 to 1720 K. *J Solid State Chem* 2005;178:2867-72. DOI
42. Goodenough JB. Electronic and ionic transport properties and other physical aspects of perovskites. *Rep Prog Phys* 2004;67:1915. DOI
43. Islam QA, Majee R, Bhattacharyya S. Bimetallic nanoparticle decorated perovskite oxide for state-of-the-art trifunctional electrocatalysis. *J Mater Chem A* 2019;7:19453-64. DOI
44. Ishihara T. Low temperature solid oxide fuel cells using LaGaO_3 -based oxide electrolyte on metal support. *J Jpn Petrol Inst* 2015;58:71-8. DOI

45. An H, Shin D, Choi SM, et al. BaCeO₃-BaZrO₃ solid solution (BCZY) as a high performance electrolyte of protonic ceramic fuel cells (PCFCs). *J Korean Ceram Soc* 2014;51:271-7. DOI
46. Kim J, Sengodan S, Kwon G, et al. Triple-conducting layered perovskites as cathode materials for proton-conducting solid oxide fuel cells. *ChemSusChem* 2014;7:2811-5. DOI
47. Shen F, Lu K. Comparison of different perovskite cathodes in solid oxide fuel cells. *Fuel Cells* 2018;18:457-65. DOI
48. Fan L, Su P. Layer-structured LiNi_{0.8}Co_{0.2}O₂: a new triple (H⁺/O²/e⁻) conducting cathode for low temperature proton conducting solid oxide fuel cells. *J Power Sources* 2016;306:369-77. DOI
49. Huang YH, Dass RI, Xing ZL, Goodenough JB. Double perovskites as anode materials for solid-oxide fuel cells. *Science* 2006;312:254-7. DOI PubMed
50. Tao S, Irvine JT. A redox-stable efficient anode for solid-oxide fuel cells. *Nat Mater* 2003;2:320-3. DOI PubMed
51. Dragan M, Enache S, Varlam M, Petrov K. Perovskite-based materials for energy applications. In: Tian H, editor. Perovskite materials, devices and integration. London: IntechOpen; 2020. DOI
52. Yousaf M, Mushtaq N, Zhu B, et al. Electrochemical properties of Ni_{0.4}Zn_{0.6}Fe₂O₄ and the heterostructure composites (Ni-Zn ferrite-SDC) for low temperature solid oxide fuel cell (LT-SOFC). *Electrochim Acta* 2020;331:135349. DOI
53. Pilania G, Kocевski V, Valdez JA, Kreller CR, Uberuaga BP. Prediction of structure and cation ordering in an ordered normal-inverse double spinel. *Commun Mater* 2020;1:84. DOI
54. Lan R, Tao S. Novel proton conductors in the layered oxide material Li_xAl_{0.5}Co_{0.5}O₂. *Adv Energy Mater* 2014;4:1301683. DOI
55. Sebastian L, Jayashree RS, Gopalakrishnan J. Probing the mobility of lithium in LISICON: Li⁺/H⁺ exchange studies in Li₂ZnGeO₄ and Li_{2+2x}Zn_{1-x}GeO₄. *J Mater Chem* 2003;13:1400-5. DOI
56. Prabhakaran K, Beigh M, Lakra J, Gokhale N, Sharma S. Characteristics of 8 mol% yttria stabilized zirconia powder prepared by spray drying process. *J Mater Process Technol* 2007;189:178-81. DOI
57. Esposito V, Gadea C, Hjelm J, et al. Fabrication of thin yttria-stabilized-zirconia dense electrolyte layers by inkjet printing for high performing solid oxide fuel cells. *J Power Sources* 2015;273:89-95. DOI
58. Park J, Lee Y, Chang I, et al. Atomic layer deposition of yttria-stabilized zirconia thin films for enhanced reactivity and stability of solid oxide fuel cells. *Energy* 2016;116:170-6. DOI
59. Lu Z, Zhou X, Fisher D, et al. Enhanced performance of an anode-supported YSZ thin electrolyte fuel cell with a laser-deposited Sm_{0.2}Ce_{0.8}O_{1.9} interlayer. *Electrochim Commun* 2010;12:179-82. DOI
60. Lee J, Lee Y, Lee H, Heo Y, Lee J, Kim J. Effect of Li₂O content and sintering temperature on the grain growth and electrical properties of Gd-doped CeO₂ ceramics. *Ceram Int* 2016;42:11170-6. DOI
61. Xu R, Wu Y, Wang X, Zhang J, Yang X, Zhu B. Enhanced ionic conductivity of yttria-stabilized ZrO₂ with natural CuFe-oxide mineral heterogeneous composite for low temperature solid oxide fuel cells. *Int J Hydrog Energy* 2017;42:17495-503. DOI
62. Liu W, Lin D, Sun J, Zhou G, Cui Y. Improved lithium ionic conductivity in composite polymer electrolytes with oxide-ion conducting nanowires. *ACS Nano* 2016;10:11407-13. DOI PubMed
63. Han M, Tang X, Yin H, Peng S. Fabrication, microstructure and properties of a YSZ electrolyte for SOFCs. *J Power Sources* 2007;165:757-63. DOI
64. Yamamoto O. Solid oxide fuel cells: fundamental aspects and prospects. *Electrochim Acta* 2000;45:2423-35. DOI
65. Anirban S, Dutta A. Structural and ionic transport mechanism of rare earth doped cerium oxide nanomaterials: effect of ionic radius of dopant cations. *Solid State Ion* 2017;309:137-45. DOI
66. Singh M, Singh AK. Studies on structural, morphological, and electrical properties of Ga³⁺ and Cu²⁺ co-doped ceria ceramics as solid electrolyte for IT-SOFCs. *Int J Hydrog Energy* 2020;45:24014-25. DOI
67. Wang B, Zhu B, Yun S, et al. Fast ionic conduction in semiconductor CeO_{2-x} electrolyte fuel cells. *NPG Asia Mater* 2019;11:51. DOI
68. Chen G, Liu H, He Y, et al. Electrochemical mechanisms of an advanced low-temperature fuel cell with a SrTiO₃ electrolyte. *J Mater Chem A* 2019;7:9638-45. DOI
69. Iwahara H, Esaka T, Uchida H, Maeda N. Proton conduction in sintered oxides and its application to steam electrolysis for hydrogen production. *Solid State Ion* 1981;3-4:359-63. DOI
70. Tao S, Irvine J. A stable, easily sintered proton-conducting oxide electrolyte for moderate-temperature fuel cells and electrolyzers. *Adv Mater* 2006;18:1581-4. DOI
71. Zuo C, Zha S, Liu M, Hatano M, Uchiyama M. Ba(Zr_{0.1}Ce_{0.7}Y_{0.2})O_{3-δ} as an electrolyte for low-temperature solid-oxide fuel cells. *Adv Mater* 2006;18:3318-20. DOI
72. Zhao Y, Zhang K, Li Y, et al. Enhanced electrocatalytic oxidation of formate via introducing surface reactive oxygen species to a CeO₂ substrate. *ACS Appl Mater Interfaces* 2021;13:51643-51. DOI
73. Scherrer B, Schlupp MV, Stender D, et al. On proton conductivity in porous and dense yttria stabilized zirconia at low temperature. *Adv Funct Mater* 2013;23:1957-64. DOI
74. Shirpour M, Gregori G, Merkle R, Maier J. On the proton conductivity in pure and gadolinium doped nanocrystalline cerium oxide. *Phys Chem Chem Phys* 2011;13:937-40. DOI PubMed
75. Stub SØ, Vøllestad E, Norby T. Mechanisms of protonic surface transport in porous oxides: example of YSZ. *J Phys Chem C* 2017;121:12817-25. DOI
76. Miyoshi S, Akao Y, Kuwata N, et al. Low-temperature protonic conduction based on surface protonics: an example of nanostructured yttria-doped zirconia. *Chem Mater* 2014;26:5194-200. DOI

77. Xing Y, Wu Y, Li L, et al. Proton shuttles in CeO₂/CeO_{2-δ} core-shell structure. *ACS Energy Lett* 2019;4:2601-7. DOI
78. Li L, Zhu B, Zhang J, Yan C, Wu Y. Electrical properties of nanocube CeO₂ in advanced solid oxide fuel cells. *Int J Hydrog Energy* 2018;43:12909-16. DOI
79. Paydar S, Zhu B, Shi J, et al. Surficial proton conducting CeO₂ nanosheets. *Ceram Int* 2023;49:9138-46. DOI
80. Morales M, Roa J, Tartaj J, Segarra M. A review of doped lanthanum gallates as electrolytes for intermediate temperature solid oxides fuel cells: from materials processing to electrical and thermo-mechanical properties. *J Eur Ceram Soc* 2016;36:1-16. DOI
81. Jaiswal N, Tanwar K, Suman R, Kumar D, Upadhyay S, Parkash O. A brief review on ceria based solid electrolytes for solid oxide fuel cells. *J Alloys Compd* 2019;781:984-1005. DOI
82. Cai Y, Chen Y, Akbar M, et al. A bulk-heterostructure nanocomposite electrolyte of Ce_{0.8}Sm_{0.2}O_{2-δ}-SrTiO₃ for low-temperature solid oxide fuel cells. *Nanomicro Lett* 2021;13:46. DOI PubMed PMC
83. Benamira M, Ringuedé A, Albin V, et al. Gadolinia-doped ceria mixed with alkali carbonates for solid oxide fuel cell applications: I. A thermal, structural and morphological insight. *J Power Sources* 2011;196:5546-54. DOI
84. Xia C, Li Y, Tian Y, et al. A high performance composite ionic conducting electrolyte for intermediate temperature fuel cell and evidence for ternary ionic conduction. *J Power Sources* 2009;188:156-62. DOI
85. Kharton V, Marques F, Atkinson A. Transport properties of solid oxide electrolyte ceramics: a brief review. *Solid State Ion* 2004;174:135-49. DOI
86. Fan L, Wang C, Chen M, Zhu B. Recent development of ceria-based (nano)composite materials for low temperature ceramic fuel cells and electrolyte-free fuel cells. *J Power Sources* 2013;234:154-74. DOI
87. Zhu B, Yun S, Lund PD. Semiconductor-ionic materials could play an important role in advanced fuel-to-electricity conversion. *Int J Energy Res* 2018;42:3413-5. DOI
88. Shi Y, Wang L, Wang Z, et al. Defect engineering for tuning the photoresponse of ceria-based solid oxide photoelectrochemical cells. *ACS Appl Mater Interfaces* 2021;13:541-51. DOI
89. Zhu B, Fan L, Mushtaq N, et al. Semiconductor electrochemistry for clean energy conversion and storage. *Electrochem Energy Rev* 2021;4:757-92. DOI
90. Fan L, Ma Y, Wang X, Singh M, Zhu B. Understanding the electrochemical mechanism of the core-shell ceria-LiZnO nanocomposite in a low temperature solid oxide fuel cell. *J Mater Chem A* 2014;2:5399-407. DOI
91. He HP, Huang XJ, Chen LQ. A practice of single layer solid oxide fuel cell. *Ionics* 2000;6:64-9. DOI
92. He H, Huang X, Chen L. Sr-doped LaInO₃ and its possible application in a single layer SOFC. *Solid State Ion* 2000;130:183-93. DOI
93. Kilner JA. Ionic conductors: feel the strain. *Nat Mater* 2008;7:838-9. DOI PubMed
94. Lee S, Zhang W, Khatkhatay F, Wang H, Jia Q, Macmanus-driscoll JL. Ionic conductivity increased by two orders of magnitude in micrometer-thick vertical yttria-stabilized ZrO₂ nanocomposite films. *Nano Lett* 2015;15:7362-9. DOI
95. Yang SM, Lee S, Jian J, et al. Strongly enhanced oxygen ion transport through samarium-doped CeO₂ nanopillars in nanocomposite films. *Nat Commun* 2015;6:8588. DOI PubMed PMC
96. Lu Y, Zhu B, Cai Y, et al. Progress in electrolyte-free fuel cells. *Front Energy Res* 2016;4:17. DOI
97. Hu H, Lin Q, Zhu Z, Zhu B, Liu X. Fabrication of electrolyte-free fuel cell with Mg_{0.4}Zn_{0.6}O/Ce_{0.8}Sm_{0.2}O_{2-δ}-Li_{0.3}Ni_{0.6}Cu_{0.07}Sr_{0.03}O_{2-δ} layer. *J Power Sources* 2014;248:577-81. DOI
98. Xia Y, Liu X, Bai Y, et al. Electrical conductivity optimization in electrolyte-free fuel cells by single-component Ce_{0.8}Sm_{0.2}O_{2-δ}-Li_{0.15}Ni_{0.45}Zn_{0.4} layer. *RSC Adv* 2012;2:3828-34. DOI
99. Zhao C, Li Y, Zhang W, et al. Heterointerface engineering for enhancing the electrochemical performance of solid oxide cells. *Energy Environ Sci* 2020;13:53-85. DOI
100. Dong W, Tong Y, Zhu B, et al. Semiconductor TiO₂ thin film as an electrolyte for fuel cells. *J Mater Chem A* 2019;7:16728-34. DOI
101. Zhu B, Lund PD, Raza R, et al. Schottky junction effect on high performance fuel cells based on nanocomposite materials. *Adv Energy Mater* 2015;5:1401895. DOI
102. Jiang SP, Wang X. Fuel cells: advances and challenges. In: Kharton VV, editor. Solid state electrochemistry II. Hoboken: Wiley; 2011. pp. 179-264. DOI
103. Fergus JW. Electrolytes for solid oxide fuel cells. *J Power Sources* 2006;162:30-40. DOI
104. Sammes N, Tompsett G, Näfe H, Aldinger F. Bismuth based oxide electrolytes - structure and ionic conductivity. *J Eur Ceram Soc* 1999;19:1801-26. DOI
105. Strickler DW, Carlson WG. Ionic conductivity of cubic solid solutions in the system CaO-Y₂O₃-ZrO₂. *J Am Ceram Soc* 1964;47:122-7. DOI
106. Dixon JM, Lagrange LD, Merten U, Miller CF, Porter JT. Electrical resistivity of stabilized zirconia at elevated temperatures. *J Electrochem Soc* 1963;110:276. DOI
107. Yeh T, Hsu W, Chou C. Mechanical and electrical properties of ZrO₂ (3Y) doped with RENbO₄ (RE = Yb, Er, Y, Dy, YNd, Sm, Nd). *J Phys IV France* 2005;128:213-9. DOI
108. Yamamoto O, Arati Y, Takeda Y, et al. Electrical conductivity of stabilized zirconia with ytterbia and scandia. *Solid State Ion* 1995;79:137-42. DOI
109. Sarat S, Sammes N, Smirnova A. Bismuth oxide doped scandia-stabilized zirconia electrolyte for the intermediate temperature solid oxide fuel cells. *J Power Sources* 2006;160:892-6. DOI
110. Hirano M, Watanabe S, Kato E, Mizutani Y, Kawai M, Nakamura Y. High electrical conductivity and high fracture strength of Sc₂O₃-doped zirconia ceramics with submicrometer grains. *J Am Ceram Soc* 1999;82:2861-4. DOI

111. Malavasi L, Fisher CA, Islam MS. Oxide-ion and proton conducting electrolyte materials for clean energy applications: structural and mechanistic features. *Chem Soc Rev* 2010;39:4370-87. DOI PubMed
112. Ishihara T, Matsuda H, Takita Y. Doped LaGaO₃ perovskite type oxide as a new oxide ionic conductor. *J Am Chem Soc* 1994;116:3801-3. DOI
113. Takahashi T, Iwahara H, Nagai Y. High oxide ion conduction in sintered Bi₂O₃ containing SrO, CaO or La₂O₃. *J Appl Electrochem* 1972;2:97-104. DOI
114. Wang X, Ma Y, Zhu B. State of the art ceria-carbonate composites (3C) electrolyte for advanced low temperature ceramic fuel cells (LTCFCs). *Int J Hydrog Energy* 2012;37:19417-25. DOI
115. Fruth V, Ianculescu A, Berger D, et al. Synthesis, structure and properties of doped Bi₂O₃. *J Eur Ceram Soc* 2006;26:3011-6. DOI
116. Shuk P, Wiemhöfer HD, Guth U, Göpel W, Greenblatt M. Oxide ion conducting solid electrolytes based on Bi₂O₃. *Solid State Ion* 1996;89:179-96. DOI
117. Steele BC, Heinzel A. Materials for fuel-cell technologies. *Nature* 2001;414:345-52. DOI PubMed
118. Mogensen M, Sammes NM, Tompsett GA. Physical, chemical and electrochemical properties of pure and doped ceria. *Solid State Ion* 2000;129:63-94. DOI
119. Shimonosono T, Hirata Y, Sameshima S, Horita T. Electronic conductivity of La-doped ceria ceramics. *J Am Ceram Soc* 2005;88:2114-20. DOI
120. Sha X, Lü Z, Huang X, et al. Study on La and Y co-doped ceria-based electrolyte materials. *J Alloys Compd* 2007;428:59-64. DOI
121. Anirban S, Dutta A. Structure and defect interaction mediated transport mechanism of mixed di-tri valent cation containing ceria-based Ionic conductors. *Int J Hydrog Energy* 2018;43:23418-29. DOI
122. Khakpour Z, Youzbashi AA, Maghsoudipour A. Influence of Gd³⁺ and Dy³⁺ co-doping and sintering regime on enhancement of electrical conductivity of ceria-based solid electrolyte. *Ionics* 2014;20:1407-17. DOI
123. Wang F, Chen S, Cheng S. Gd³⁺ and Sm³⁺ co-doped ceria based electrolytes for intermediate temperature solid oxide fuel cells. *Electrochem Commun* 2004;6:743-6. DOI
124. Rai A, Mehta P, Omar S. Ionic conduction behavior in Sm_xNd_{0.15-x}Ce_{0.85}O_{2-δ}. *Solid State Ion* 2014;263:190-6. DOI
125. Tadokoro S, Muccillo E. Effect of Y and Dy co-doping on electrical conductivity of ceria ceramics. *J Eur Ceram Soc* 2007;27:4261-4. DOI
126. Lin Y, Fang S, Su D, Brinkman KS, Chen F. Enhancing grain boundary ionic conductivity in mixed ionic-electronic conductors. *Nat Commun* 2015;6:6824. DOI PubMed PMC
127. Ramesh S, James Raju K. Preparation and characterization of Ce_{1-x}(Gd_{0.5}Pr_{0.5})_xO₂ electrolyte for IT-SOFCs. *Int J Hydrog Energy* 2012;37:10311-7. DOI
128. Arunkumar P, Preethi S, Suresh Babu K. Role of iron addition on grain boundary conductivity of pure and samarium doped cerium oxide. *RSC Adv* 2014;4:44367-76. DOI
129. Zajac W, Suescun L, Świerczek K, Molenda J. Structural and electrical properties of grain boundaries in Ce_{0.85}Gd_{0.15}O_{1.925} solid electrolyte modified by addition of transition metal ions. *J Power Sources* 2009;194:2-9. DOI
130. Kang YJ, Choi GM. The effect of alumina and Cu addition on the electrical properties and the SOFC performance of Gd-doped CeO₂ electrolyte. *Solid State Ion* 2009;180:886-90. DOI
131. Zhu B, Yang X, Xu J, et al. Innovative low temperature SOFCs and advanced materials. *J Power Sources* 2003;118:47-53. DOI
132. Raza R, Wang X, Ma Y, Liu X, Zhu B. Improved ceria-carbonate composite electrolytes. *Int J Hydrog Energy* 2010;35:2684-8. DOI
133. Zhang G, Li W, Huang W, et al. Strongly coupled Sm_{0.2}Ce_{0.8}O₂-Na₂CO₃ nanocomposite for low temperature solid oxide fuel cells: one-step synthesis and super interfacial proton conduction. *J Power Sources* 2018;386:56-65. DOI
134. Zhu B, Li S, Mellander B. Theoretical approach on ceria-based two-phase electrolytes for low temperature (300-600 °C) solid oxide fuel cells. *Electrochem Commun* 2008;10:302-5. DOI
135. Zhu B. Intermediate temperature proton conducting salt-oxide composites. *Solid State Ion* 1999;125:397-405. DOI
136. Zhu B. Next generation fuel cell R&D. *Int J Energy Res* 2006;30:895-903. DOI
137. Maier J. Ionic conduction in space charge regions. *Prog Solid State Chem* 1995;23:171-263. DOI
138. Schober T. Composites of ceramic high-temperature proton conductors with inorganic compounds. *Electrochem Solid-State Lett* 2005;8:A199. DOI
139. Huang J, Gao Z, Mao Z. Effects of salt composition on the electrical properties of samaria-doped ceria/carbonate composite electrolytes for low-temperature SOFCs. *Int J Hydrog Energy* 2010;35:4270-5. DOI
140. Riess I, Gödickemeier M, Gauckler LJ. Characterization of solid oxide fuel cells based on solid electrolytes or mixed ionic electronic conductors. *Solid State Ion* 1996;90:91-104. DOI
141. Lu Y, Zhu B, Wang J, Zhang Y, Li J. Hybrid power generation system of solar energy and fuel cells: hybrid power generation system. *Int J Energy Res* 2016;40:717-25. DOI
142. Zhu B, Fan L, Lund P. Breakthrough fuel cell technology using ceria-based multi-functional nanocomposites. *Appl Energy* 2013;106:163-75. DOI
143. Zhu B, Ma Y, Wang X, Raza R, Qin H, Fan L. A fuel cell with a single component functioning simultaneously as the electrodes and electrolyte. *Electrochem Commun* 2011;13:225-7. DOI

144. Zhu B, Raza R, Qin H, Fan L. Single-component and three-component fuel cells. *J Power Sources* 2011;196:6362-5. [DOI](#)
145. Dong X, Tian L, Li J, Zhao Y, Tian Y, Li Y. Single layer fuel cell based on a composite of $Ce_{0.8}Sm_{0.2}O_{2-\delta}$ - Na_2CO_3 and a mixed ionic and electronic conductor $Sr_2Fe_{1.5}Mo_{0.5}O_{6-\delta}$. *J Power Sources* 2014;249:270-6. [DOI](#)
146. Paydar S, Peng J, Huang L, et al. Performance analysis of $LiAl_{0.5}Co_{0.5}O_2$ nanosheets for intermediate-temperature fuel cells. *Int J Hydrog Energy* 2021;46:26478-88. [DOI](#)
147. Zhou Y, Guan X, Zhou H, et al. Strongly correlated perovskite fuel cells. *Nature* 2016;534:231-4. [DOI](#)
148. Akbar N, Paydar S, Afzal M, et al. Tuning tin-based perovskite as an electrolyte for semiconductor protonic fuel cells. *Int J Hydrog Energy* 2022;47:5531-40. [DOI](#)
149. Dong W, Yaqub A, Janjua NK, Raza R, Afzal M, Zhu B. All in one multifunctional perovskite material for next generation SOFC. *Electrochim Acta* 2016;193:225-30. [DOI](#)
150. Meng Y, Mi Y, Xu F, et al. Low-temperature fuel cells using a composite of redox-stable perovskite oxide $La_{0.7}Sr_{0.3}Cr_{0.5}Fe_{0.5}O_{3-\delta}$ and ionic conductor. *J Power Sources* 2017;366:259-64. [DOI](#)
151. Akbar N, Paydar S, Wu Y. Tuning an ionic-electronic mixed conductor $NdBa_{0.5}Sr_{0.5}Co_{1.5}Fe_{0.5}O_{5+\delta}$ for electrolyte functions of advanced fuel cells. *Int J Hydrog Energy* 2021;46:9847-54. [DOI](#)
152. Tu Z, Tian Y, Liu M, et al. Remarkable ionic conductivity in a LZO-SDC composite for low-temperature solid oxide fuel cells. *Nanomaterials* 2021;11:2277. [DOI](#) [PubMed](#) [PMC](#)
153. Shah MY, Lu Y, Mushtaq N, et al. ZnO/MgZnO heterostructure membrane with type II band alignment for ceramic fuel cells. *Energy Mater* 2022;2:200031. [DOI](#)
154. Lu Y, Zhu B, Shi J, Yun S. Advanced low-temperature solid oxide fuel cells based on a built-in electric field. *Energy Mater* 2021;1:100007. [DOI](#)
155. Mahato N, Banerjee A, Gupta A, Omar S, Balani K. Progress in material selection for solid oxide fuel cell technology: a review. *Prog Mater Sci* 2015;72:141-337. [DOI](#)
156. Kang S, Lee J, Cho GY, et al. Scalable fabrication process of thin-film solid oxide fuel cells with an anode functional layer design and a sputtered electrolyte. *Int J Hydrog Energy* 2020;45:33980-92. [DOI](#)
157. Yang Y, Zhang Y, Yan M. A review on the preparation of thin-film YSZ electrolyte of SOFCs by magnetron sputtering technology. *Sep Purif Technol* 2022;298:121627. [DOI](#)
158. Wang B, Cai Y, Xia C, et al. Semiconductor-ionic membrane of LaSrCoFe-oxide-doped ceria solid oxide fuel cells. *Electrochimica Acta* 2017;248:496-504. [DOI](#)
159. Hu E, Jiang Z, Fan L, et al. Junction and energy band on novel semiconductor-based fuel cells. *iScience* 2021;24:102191. [DOI](#) [PubMed](#) [PMC](#)
160. Harboe S, Schreiber A, Margaritis N, Blum L, Guillon O, Menzler N. Manufacturing cost model for planar 5 kWel SOFC stacks at Forschungszentrum Jülich. *Int J Hydrog Energy* 2020;45:8015-30. [DOI](#)
161. Dubois A, Ricote S, Braun RJ. Benchmarking the expected stack manufacturing cost of next generation, intermediate-temperature protonic ceramic fuel cells with solid oxide fuel cell technology. *J Power Sources* 2017;369:65-77. [DOI](#)